The Thesis Committee for Taylor Marie Borgfeldt
Certifies that this is the approved version of the following thesis:

Crustal seismic velocity models of Texas

APPROVED BY
SUPERVISING COMMITTEE:

Supervisor:

Cliff Frohlich

Co-Supervisor:

Jacob I. Walter

Luc Lavier

Stephen P. Grand

Crustal seismic velocity models of Texas

by

Taylor Marie Borgfeldt

Thesis

Presented to the Faculty of the Graduate School of

The University of Texas at Austin

in Partial Fulfillment

of the Requirements

for the Degree of

Master of Science in Geological Sciences

The University of Texas at Austin

August 2017

Dedication

I would like to dedicate my thesis to my mom who taught me what a work ethic is. Thank you to John who always supported me and helped me stay true to my goals and aspirations. I would also like to thank Bubba for the guidance and honest edits.

Acknowledgements

Thank you to Dr. Jake Walter and Dr. Cliff Frohlich for their advising throughout my Master's degree and for taking me on as their first and last student, respectively. Many thanks to Dr. Jake Walter and the Bureau of Economic Geology for funding my position as a graduate research assistant and for the financial support for tuition from the Jackson School of Geosciences.

Appreciation goes out to the scientists of TexNet and CISR who provided me with data and resources to complete my research.

Thanks to Marcy Davis for the continued support and office chats throughout my degree. I appreciate the guidance Dr. Steve Grand and Dr. Luc Lavier provided both in the classroom and on my work. I am also grateful to the UTIG administration and Philip Guerrero for providing such timely assistance during my time at UT.

The facilities of IRIS Data Services, and specifically the IRIS Data Management Center, were used for access to waveforms, related metadata, and/or derived products used in this study. IRIS Data Services are funded through the Seismological Facilities for the Advancement of Geoscience and EarthScope (SAGE) Proposal of the National Science Foundation under Cooperative Agreement EAR-121681. Thank you to the Bureau of Economic Geology at the University of Texas at Austin for providing a database of sonic logs.

Abstract

Crustal seismic velocity models of Texas

Taylor Marie Borgfeldt, M.S.GEO.SCI.

The University of Texas at Austin, 2017

Supervisor: Cliff Frohlich

Co-Supervisor: Jacob I. Walter

Our investigation distinguishes six distinct geologic regions within Texas and determines a preferred one-dimensional (1D) crustal structure for each. These models, which consist of flat layers of varying thicknesses and constant P and S-wave velocities in each layer, represent the best average crustal velocity structure. Our investigation is motivated by TexNet, a new statewide seismograph network, which will need more accurate regional crustal models to better locate earthquakes throughout the state.

We test previously published models as well as newly generated models. The data used to develop the new models include previously used velocity models, geologic cross sections, refraction and reflection studies, sonic logs, receiver function results and any other geophysical survey information available for the specific regions.

We test the accuracy of the various regional models by relocating earthquakes with Hypoinverse1.40 (HYPO1.40). The earthquake catalogs vary by region but meet standard criteria for quantity and quality of phases recorded. We relocate each set of regional earthquakes with all previously published and newly generated models and determine the

preferred model by lowest RMS (root mean square) residuals, i.e., the differences in recorded and modeled travel times. To understand which layers most significantly affect observed travel times, we perform source-to-station ray tracing for available regional earthquakes with magnitudes larger than M2.6. We also use the arrival data to plot Wadati diagrams and find the regional Vp/Vs ratio, which is applied to the preferred P-velocity model to determine a preferred S-velocity model.

Our data allow us to determine new preferred velocity models for four of the six regions (East Texas, Fort Worth Basin, Panhandle, and West Texas) and confirm a previously published model for two regions (Central and Gulf Coastal Plain). Central Texas does not have enough earthquake data or geophysical studies to determine a new model, so we suggest the continued use of the Mitchell and Landisman (1971) velocity model until new seismic data is available. The velocity model published by Cram, Jr. (1961) is the preferred model for regional earthquake location for the Gulf Coastal Plain.

Table of Contents

List of Tables

List of Figures

Chapter 1: Introduction

Seismologists commonly use 1D velocity models to locate earthquake hypocenters because it is computationally fast. Rapidly determined, accurate locations are important for networks that provide real-time earthquake information. TexNet, a state government funded seismic monitoring program, will record seismicity that occurs in Texas and report the earthquakes through an online database. This thesis is a study of previously used and newly generated velocity models of Texas that aims to provide a complete set of regional models for the location of earthquakes recorded by the TexNet network.

Although several investigations have accurately located Texas earthquakes' epicenters of local events using temporary or regional networks of seismograph stations, most Texas earthquakes have relatively low magnitudes and can't be located with a high level of accuracy due to a widely spaced seismic network (~70 km station spacing during US Transportable Array and >160 km in TexNet network). Calculating an earthquake hypocenter requires a seismic velocity for the crust and upper mantle to accurately calculate the travel time from hypocenter to seismometer. If the velocity model is inaccurate, results could lead to an inaccurate location for the event. To fully understand the seismicity in Texas and have high confidence in the hypocenters of future events, the preferred models provided in this thesis produce low RMS values for the regional earthquakes tested and are a reasonable representation of the regional crustal structure.

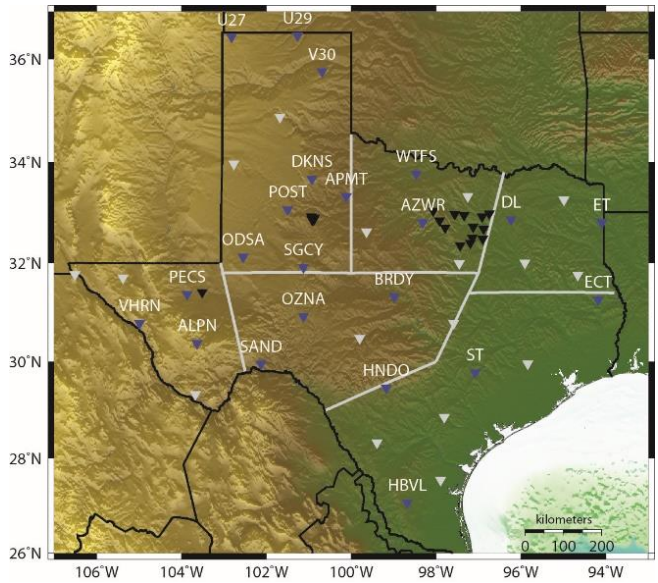

Figure 1: Map of permanent seismograph stations operating in 2015 (grey) and proposed and installed locations for the 22 permanent (blue) and 19 auxiliary (black) TexNet stations in Texas. Labels are station codes. Grey lines are boundaries of geographic regions evaluated in this study (Figure 4).

Prior to the Center for Integrated Seismicity Research (CISR) program, earthquakes in Texas were located by the U.S. Geological Survey and in independent studies that utilized a variety of velocity models determined specifically for each study (Cram, Jr., 1961; Hales, Helsley and Nation, 1970; Frohlich, 2012; Frohlich and Brunt, 2013; Gan and Frohlich, 2013; Frohlich *et al.*, 2014; Hornbach *et al.*, 2015; Walter *et al.*, 2016). Currently being deployed, TexNet will be a statewide network of 22 permanent and 19 auxiliary stations with an average station spacing greater than 160 km between permanent stations. This large station spacing means the first arrivals recorded at stations will likely be from the rays that travel through deeper, higher velocity layers before reaching the seismometer. To ensure we capture the relevant velocity structure that impacts travel time, we refine the velocity models from the surface to the Mohorovicic Boundary.

Chapter 2: Regionalization

The majority of Texas's geologic basement is part of the continental craton of the contiguous United States, an igneous and metamorphic unit deposited during the Precambrian, forming Laurentia (Figure 2) (Ewing, 1991) Throughout Texas, above the Precambrian basement is an unconformity separating the basement and the Ordovician-aged karstic limestone Ellenburger formation. The eastern boundary of the Precambrian basement and Ellenburger is the Ouachita Tectonic Front (Figure 3). South of the front, the rifted Paleozoic continental crust formed the Gulf Coastal Plain. We use these three units (Precambrian crust, Paleozoic crust, Ellenburger limestone), as key velocity layers in our models because the depth and extent are well mapped and the units continue between regions. Above these main units, the geology varies by region and basin with independent geologic units that compose the surface and shallow crustal geology. The heterogeneous crust across the state is correlated with diverse crustal seismic velocity structures. To approximately represent the average crustal structure, we divide Texas into six regions based on geologic and tectonic boundaries (Figure 4): 1) East Texas; 2) Fort Worth Basin (FWB); 3) Central Texas; 4) Gulf Coastal Plain (GCP); 5) Panhandle; 6) West Texas.

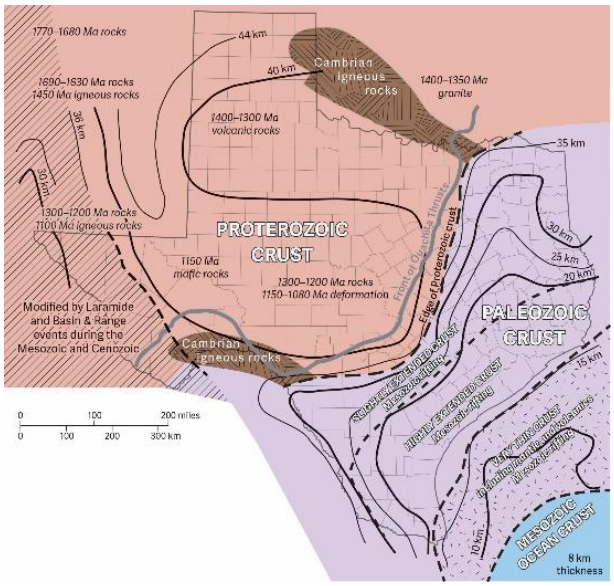

Figure 2: Map of principle crustal provinces of Texas. The two major provinces are the Proterozoic crust of West and North Texas, and the Paleozoic crust to its southeast that was extended in the Mesozoic. The map also indicates areas modified by later events. Numbered black lines indicate the approximate crustal thickness. Figure from Sawyer, Buffler and Pilger (1991) and republished with permission from the Bureau of Economic Geology.

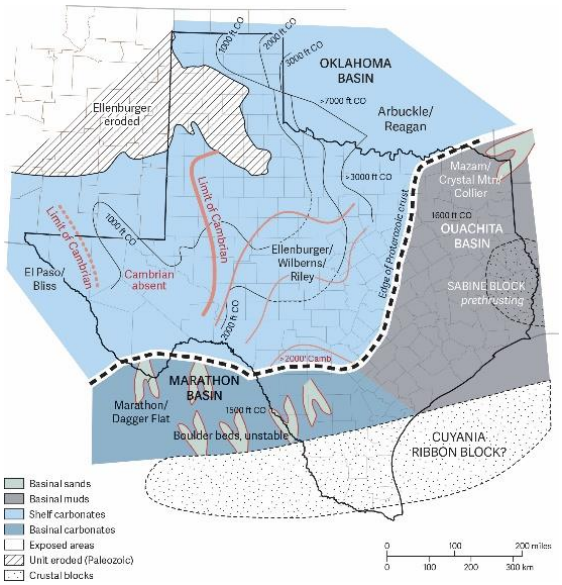

Figure 3: Map of deposits in Texas between Late Cambrian to Early Ordovician. The three major provinces are the Ellenburger shelf carbonates, the Ouachita Basin basinal muds and the basinal carbonates in the Marathon Basin. Figure from Sawyer, Buffler and Pilger (1991) and republished with permission from the Bureau of Economic Geology. Black dashed line marks the boundary between Proterozoic and Paleozoic crust, as shown in Figure 2.

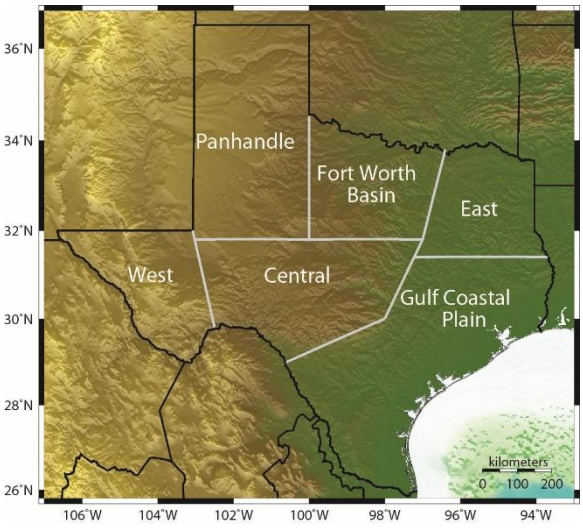

Figure 4: The six geographic regions of Texas (grey lines are boundaries) evaluated in this study to develop 1D velocity models for locating earthquakes within each region.

2.1 EAST TEXAS

The East Texas region contains the East Texas Basin and the structural features that form the boundaries of the basin (Talco Fault Zone, Mexia Fault Zone, and Angelina Flexure). The basement of this region is the Paleozoic rifted crust (Figure 2) and the eastern limit is the Ouachita Tectonic Front. Above the rifted crust, the Jurassic aged Louann Salt was deposited into the basin. Subsequent carbonate units were deposited in laminar, continuous layers with no tectonic activity within the basin. Later deformation occurred within the basin by halokinesis, gravitationally induced creep of salt (Jackson, 1982; Hammes and Frébourg, 2012). The Louann Salt intersects laminar layers above its original planar deposition in pillows and diapirs that were mobilized post rifting of the passive margin of the Gulf Coastal Plain (Jackson, 1982; Ewing, 1991; Hammes and Frébourg, 2012).This means the flat layer velocity models used for earthquake location are accurate aside from the salt diapirs.

The East Texas region, historically, had not experienced much seismicity until the M_W4.8 event in Timpson, Texas on 17 May 2012 (Frohlich *et al.*, 2014). To investigate this earthquake, Frohlich *et al.* (2014) developed a velocity model tuned to regional geology (Table A1) and based loosely on the WUS (western U.S.) model used by Hermann, Benz and Ammon (2011). Walter *et al.* (2016) (Table A2) located events in northern Louisiana and East Texas with an updated version of the Frohlich et al. (2014) model (Table A1).

The western boundary of the East region is the Ouachita Tectonic Front. The southern boundary, approximately 31.5^{o}N, is aligned with the trend of the base of Austin Chalk that is 2 to 4 km deep. The eastern and northern boundaries are the Louisiana and Oklahoma state lines, respectively.

2.2 FORT WORTH BASIN (FWB)

Since 2008, the FWB has experienced a high level of seismic activity, providing a large catalog of seismic events to refine and test our regional velocity models.

The stratigraphic units of the FWB are thin layers of Cretaceous rocks, 1.8-2 km of Pennsylvanian clastics and carbonates, 1.2-1.5 km of Ordovician to Mississippian carbonates and shales, followed by sedimentary rocks that get as thick as 3.7 km near the Muenster Arch. Below these basin specific units, the Ellenburger and Precambrian granitic basement are present. The FWB's deepest point is in the northeast, shallowing to the southwest, with the uplift of the Precambrian basement in the Llano Uplift.

SMU seismologists generously provided regional velocity models used in earthquake locations of various areas in the Dallas-Fort Worth (DFW) metroplex (Tables S3-S7). We also use Hornbach et al. (2015), Justinic et al. (2013), and Frohlich et al. (2011) and (2013) velocity models as reference models for the FWB (Tables S8-S11).

The western boundary of the FWB is 100°W (USGS Boundary of the Bend Arch – Fort Worth Basin Province). The eastern boundary is the Ouachita Tectonic Front. The southern boundary, approximately 32°N, separates the shallowing geology of the FWB from the Llano Uplift and Central Texas geology. The northern boundary is the Texas-Oklahoma state line.

2.3 CENTRAL TEXAS

During the Mesozoic Era, Central Texas's limestone and chalk units were deposited in the marine seas of the Cretaceous seaway. These units are continuous and exposed throughout the Central Texas region and overlain by more modern alluvium. The Llano Uplift is an anomalous portion of the region, a domal uplift of the Precambrian granitic basement in the eastern portion of the Central Texas region. Because there is lower oil and gas activity in this region, there are few sonic logs in the Bureau of Economic Geology's database within the Central Texas region to control shallow velocity structure. The eastern and southern boundaries follow the Ouachita Tectonic Front. The northern boundary separates the Central Texas geology from the FWB and Panhandle regional geology, approximately along 32°N. The western boundary parallels the Delaware Basin to separate the regional geology of West and Central Texas.

Frohlich *et al*. (2013) found the Mitchell and Landisman (1971) Manitou southwest Oklahoma model (Table A12) produced low residuals for the Eagle Ford events that were recorded at the TA stations for events in the northern area of their study region. Since the Eagle Ford has the most similar geology to the Central Texas region, we use the Mitchell and Landisman (1971) model as our reference model for this region.

2.4 Gulf Coastal Plain

The GCP, a rifted continental margin, contains thick Mesozoic and Cenozoic sedimentary packages, comprised mostly of carbonates and clastics deposited from the Jurassic to Cretaceous (Ewing, 2016). Below the Mesozoic and Cenozoic rocks lies the Paleozoic Ouachita orogenic belt (Keller and Shurbet, 1975). The crustal thickness beneath the GCP ranges from 35 to 10 km, creating a large velocity contrast within the region (Harry and Londono, 2004).

We use two crustal models as reference models in the GCP. The first is Cram, Jr.'s (1961) velocity model (Table A13) from a crustal refraction survey along the GCP. The second reference model is the tripartite 3 model derived by Keller and Shurbet (1975) (Table A14) from Rayleigh wave dispersion data. Frohlich *et al.*'s (2012) study of the Alice seismicity and the Frohlich and Brunt (2013) study of the Eagle Ford events both use the Keller and Shurbet (1975) model.

The northern boundary of the GCP is the Ouachita Tectonic Front and the southern extent of the East Texas Basin (Angelina Flexure). The remaining boundaries of the GCP region are formed by the Gulf of Mexico and state lines.

2.5 Panhandle

The overall geologic structure of the Panhandle, eastern New Mexico and western Oklahoma are similar (Stewart and Pakiser, 1962; Tryggvason and Qualls, 1967; Ewing, 2016). We therefore use data sets from New Mexico and Oklahoma to investigate the preferred velocity structure for the Panhandle.

Above the continental crust, Paleozoic units of various marine environments were deposited (Ewing, 2016), including the Ellenburger formation. Above the Ellenburger are carbonates with interbedded shale, limestone, dolomite and dolomitic limestone. Because the Ellenburger unit was eroded by the uplift of the Texas Arch, the Palo Duro Basin is the only basin missing the Ellenburger within the areal extent of the Ellenburger. We still use the Ellenburger unit as a velocity layer in our models because it is present in the majority of the Panhandle region. Along with the Palo Duro Basin and Anadarko Basin, the Midland Basin stretches across the southwestern area of the Panhandle.

Our reference models for the Panhandle include the Chelsea model, described by Mitchell and Landisman (1971), and Ewing's (1991) Midland Basin model (Table A15 and S16). Gan and Frohlich's (2013) analysis of the Snyder-Cogdell earthquakes used the original Chelsea model (Table A15), but our study removed the two low-velocity zones (LVZs) from the Chelsea model. The Ewing (1991) velocity model is published as a cross-section of the Midland Basin (Table A16). For our study, we approximate layer thickness from the cross-section and remove the LVZ.

The southern boundary (approximately 32°N) separates the Panhandle and Central Texas regional geologies. The remaining boundaries are formed by state lines.

2.6 West Texas

West Texas is geologically complex, containing the Chihuahua Tectonic Belt, Delaware Basin, Midland Basin, Central Basin Platform, Basin and Range region, and volcanic deposits. This region experienced a transgressive then regressive marine sequence during the Mesozoic. The Laramide compression uplifted mountains along the southern border between Texas and Mexico.

The Delaware Basin and the Central Basin Platform (CBP) form the largest geologic structures within the West Texas region. The Midland Basin, geologically similar to the Delaware Basin, is within the Panhandle region. All three features have the Precambrian basement and Ellenburger karstic limestone at the base, but when the CBP was uplifted, deep erosion occurred and truncated sediments to as early as the Precambrian

(Orr, 1984). The Delaware Basin has approximately seven km of sediments, and CBP and Midland Basin have approximately three km (Doser *et al.*, 1992).

Our reference models for West Texas include the model published in Orr (1984), which is Gulf Oil Corporation's check-shot data from the Keystone region of the Central Basin Platform (Table A18). We also test Ewing's (1991) Delaware Basin model and Stewart and Pakiser's (1962) GNOME model from eastern New Mexico (Tables S17 and S19).

The eastern boundary of West Texas parallels the boundary between the CBP and Midland Basin and separates West and Central Texas regional geology. The remaining boundaries are formed by state lines.

Chapter 3: Methods

The reference velocity models described in the previous section (Tables S1-S19) serve as the basis for revisions and determining preferred models in each of the six regions. We modify the existing velocity models and build new models with an integration of *a priori* data, including both geologic and geophysical data sets. For each of the six regions described in Chapter 2, we evaluate sonic logs, geophysical refraction and reflection surveys, and, to measure regional crustal thickness, the EarthScope Automated Receiver Survey (EARS) from Incorporated Research Institutions for Seismology (IRIS) (Crotwell and Owens, 2005). We then iteratively modify these models, testing them by comparing observed and calculated travel times for representative earthquakes and by locating regional earthquakes using the program Hypoinverse1.40 (HYPO1.40). Modified models that produced better agreement between observed and calculated phase arrivals were deemed superior.

3.1 Sonic Logs

Sonic logs (Figure 5, Appendix 3.1) are a well logging tool that record the P-velocity of the rock units surrounding the borehole. The velocity of the rock units is calculated by measuring the travel time between the transmitter to receiver, both on the same sonic logging tool. These logs are commonly used for oil and gas exploration and typically extend to an average depth of 5 km. These measurements give point control on the velocity structure within the shallow crust. The sonic logs used in this study are from petroleum and industry documents archived by the Bureau of Economic Geology at the University of Texas at Austin and are selected based on: 1) clarity of the scanned log; 2) depth coverage; and 3) location. We use a software package, NeuraLog, to digitize three or more scanned logs per region (Figure 5) with the intention of measuring shallow crust velocity structure (surface to approximately five km). After digitizing, we calculate a

moving average on the digitized logs and block velocities to incorporate into our 1D velocity models. We then compare these velocity packages to geologic units and previous velocity studies to ensure consistency between studies.

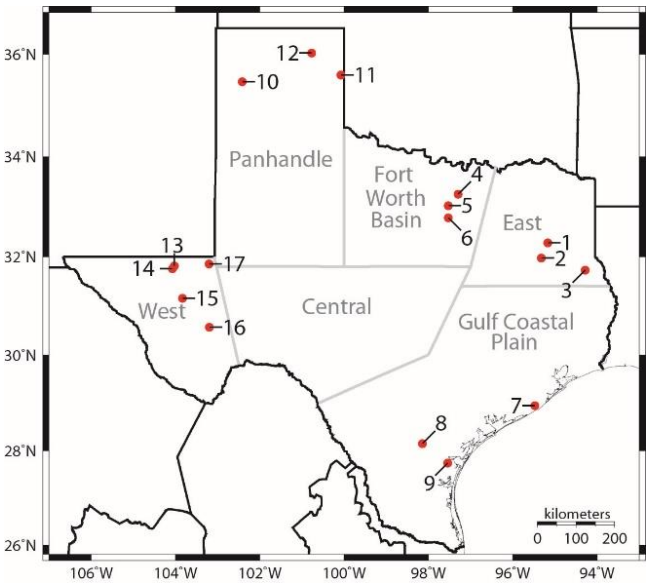

Figure 5: Locations of sonic logs (black circles; Table B1) traced and used in this study to modify shallow crustal velocities. Grey lines mark regional boundaries.

3.2 EARTHSCOPE AUTOMATED RECEIVER SURVEY

The EarthScope Automated Receiver Survey (EARS) data set by Incorporate Research Institutions for Seismology (IRIS) is used to measure regional crustal thickness (Crotwell and Owens, 2005). EARS is a fully automated receiver function data product that measured crustal thickness when the US Transportable Array (TA) was deployed in Texas from 2008-2010. Receiver function analysis evaluates P-waves from teleseismic earthquakes that impinge on the base of the crust, and subsequent P-to-S and S-to-P conversions at crustal layer boundaries, to determine crustal structure beneath a seismic station. In this investigation we use the EARS results to assess total crustal thickness.

For our regional velocity models, the depth to Moho for each region is the average of the crustal thickness at each TA station within the respective region. We use a uniform halfspace, which is a unit with no bottom depth specified, for the mantle.

3.3 GENERATING MODELS

To produce new velocity models, we collect the available regional data discussed above to generate revised versions of reference models described in Chapter 2 as well as new models; the new models include layers from the available reference models. After preliminary RMS tests (see 3.4 RMS Tests of Models with Hypoinverse1.40) of the initial velocity models in HYPO1.40, we ray trace (see 3.5 Ray tracing Models) the models with lowest RMS values to analyze the layers which are significant for travel time. We then modify those significant layers' thicknesses or velocities and continue to iteratively test and modify velocity models, with the goal of selecting a preferred velocity model in each geographic region.

3.4 RMS TESTS OF MODELS WITH HYPOINVERSE1.40

To evaluate the new and revised versions of the reference models, we use Hypoinverse 1.40 (HYPO1.40) (Klein, 2014) to test the accuracy of the regional velocity models by locating regional earthquakes that meet the following criteria: 1) all phases are analyst-picked; 2) a minimum of eight P arrival readings; 3) at least one S arrival reading; and 4) gap angle less than 180°, (Husen *et al.*, 1999; Husen, Kissling and Clinton, 2011). These criteria produced a total of 782 events statewide to test our models (Table 1) (Figure 6). However, to increase spatial coverage of earthquakes in the FWB, we decrease the P-arrival criterion to five phases. The change in criteria did not increase RMS values for the regional events, but it did allow us to test the Moho halfspace velocity. Central Texas only

had eight events that occurred in the region, but we do not have enough high-quality phases recorded to build a phase file for the region. Therefore, we do not test velocity models for this region.

HYPO1.40 is an earthquake location program that locates earthquakes using recorded arrival times of P and S-phases. It uses an iterative least-square technique that linearizes the travel-time vs distance function at each location step, converging on a location which is a local minimum of the root-mean-square (RMS) of the travel time residuals, r, i.e. the differences squared between the observed (t_i^o) and calculated (t_i^c) arrival times at seismograph stations (Equation 1). The calculated travel time produced by HYPO1.40 is a function of the earthquake source parameters and velocity model.

1) $r = t_i^o - t_i^c$

Due to the large station spacing of the TA stations (~70 km) in place during the seismicity we use to test our velocity models in comparison to the depth of earthquakes in most of Texas, the event focal depths cannot be well constrained with our velocity models and phase arrivals. Therefore, we locate the regional earthquakes using a fixed-depth of 5 km for the East, FWB, GCP and Panhandle regions. The fixed-depth ensures the velocity models accurately locate earthquake epicenters without accommodating the error by adjusting the depth. We use free-depths for West Texas because there is known shallow and deeper tectonic seismic activity along with a large number events that meet our criteria and are evenly distributed across the region (Figure 6). The quality of the earthquake data in West Texas allows us to have high confidence in the locations calculated by HYPO1.40 using our velocity models. After locating the events, we throw out events that do not locate or have a horizontal error (ERH) > 10 km (fixed-depth only) and update our phase file.

Figure 6 shows all events used for RMS tests. As an example, we show the station coverage and available earthquake data for East Texas and West Texas (Figure 7 and 8) for comparison, but the maps of station coverage and earthquake data for the other four regions are in S3.4.

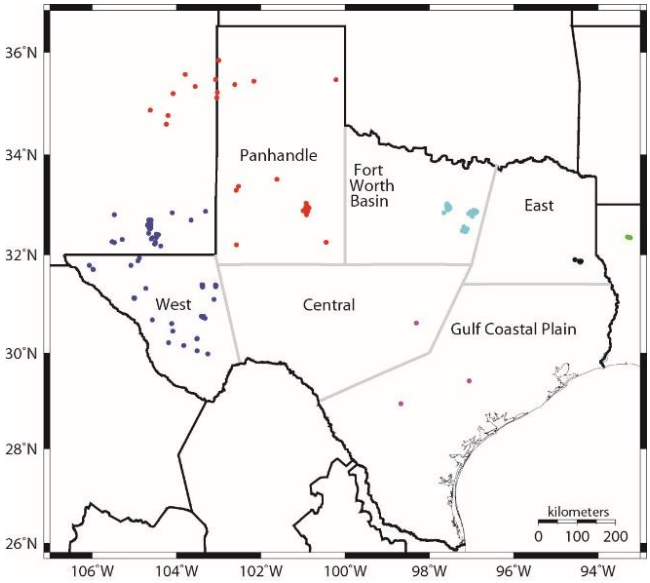

Figure 6: Map showing all regional earthquakes used in location tests to assess regional velocity models. The blue circles are earthquakes used in West Texas tests, red circles are Panhandle events, turquoise circles are FWB events, green circles are East Texas events, purple circles are GCP events, and black circles are events used in both East Texas and GCP tests.

	Central	East	Fort Worth Basin	Gulf Coastal Plain	Panhandle	West
Regional Events	n/a	8	616	7	51	100
P-Phase	n/a	98	6,557	125	834	1,638
S-Phase	n/a	92	5,283	107	782	1,460

Table 1: Number of regional events, P and S-phases used to test velocity models with HYPO1.40

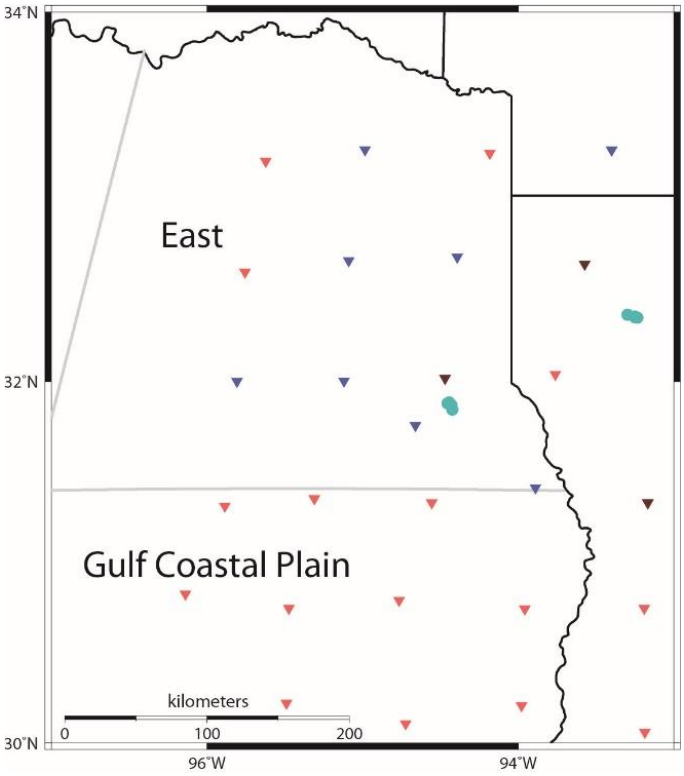

Figure 7: Map of the East Texas region showing 7 earthquakes (blue circles) and seismograph stations (triangles) used for location test to assess regional velocity models. Earthquakes are events that occurred 2010-2012 having analyst-picked P and S-phases on records from TA stations, with epicenters determined using the Borgfeldt East model (Table 3). The triangles are seismograph stations that recorded phases for the mapped events (pink – fewer than 5 P-phases recorded; blue – 5-10 P-phases; maroon – 10-15 P-phases).

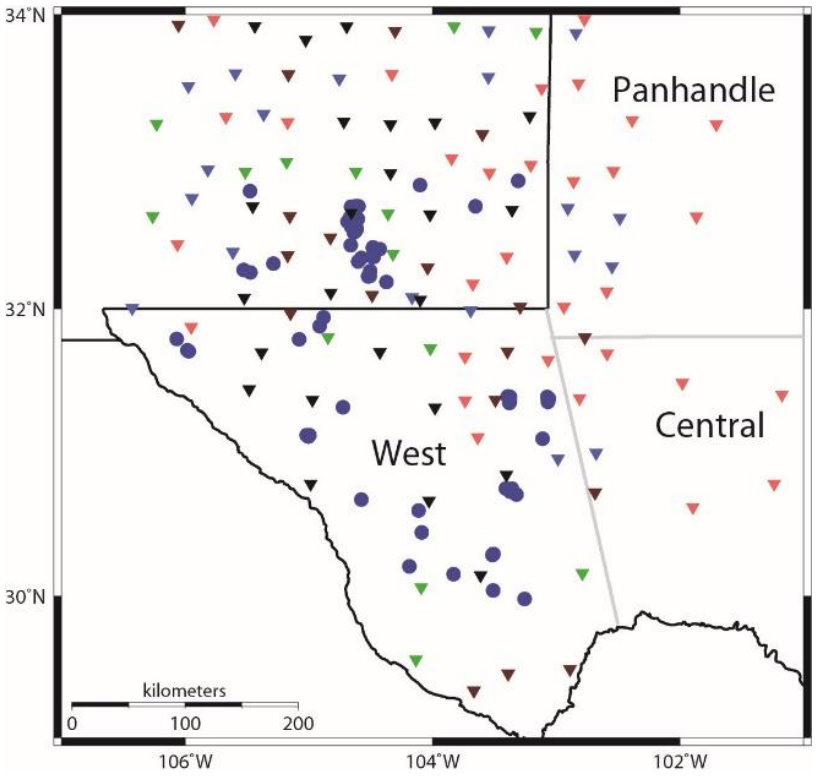

Figure 8: Map of the West Texas region showing 100 earthquakes (blue circles) and seismograph stations (triangles) used for location test to assess regional velocity models. Earthquakes are events that occurred 2010-2012 having analyst-picked P and S-phases on records from Transportable Array stations, with epicenters determined using the Borgfeldt West Texas model (Table 7). The triangles are seismograph stations that recorded phases for the mapped events (pink – fewer than 5 P-phases recorded; blue – 5-10 P-phases; maroon – 10-15 P-phases; green – 15-20 P-phases; black – greater than 20 P-phases).

East Texas has eight events that meet the earthquake criteria, but four of the earthquakes are located in Louisiana. We still use these for our RMS tests because the geology and crustal structure does not change at the state boundary. As shown in Figure 7, the 13 events that meet the criteria occurred in clusters on the eastern half of the region. Due to the station spacing when seismicity occurred, gap angle is the limiting factor for the events in East Texas. East Texas is an example of limited seismic data and coverage.

In comparison to East Texas, West Texas has a large number of events (100) that meet the criteria for earthquakes. The events are distributed across the region with well-distributed station coverage. We include the events that occurred in New Mexico south of 33^0N because the geology is continuous into New Mexico.

3.5 RAY TRACING MODELS

To further test the accuracy of the models, we evaluate the travel times from selected earthquakes by comparing observed arrival times with arrivals calculated by ray tracing; the ray tracing allows us to determine which model velocity layers most influence times in different distance ranges. The first step in this process is finding at least one regional earthquake that has a large enough magnitude (M_W>2.6) to be seen clearly at stations over 200 km distance and has a credible hypocenter and origin time published in a peer-reviewed publication (Frohlich *et al.*, 2011; Frohlich, 2012; Justinic *et al.*, 2013; Hornbach *et al.*, 2015; Walter *et al.*, 2016). We then chose a transect of stations extending in an azimuthal direction from nearby the event to several hundred kilometers away, with the intention of sampling each layer of the velocity model that has a first arrival predicted by ray tracing.

The inputs for the ray tracing program include an earthquake depth, range of station spacing (km) and a 1D velocity model. The depth is equal to the hypocenter location found in the respective study that located the event. The station spacing is a broad range that includes stations in place during the event; typically the range is 10 to 300 km. The velocity models with the lowest residuals in HYPO1.40 (Tables 3-7) serve as the input for the ray tracing program to find the calculated travel time (t_i^c) to test how the modelled times compare to the observed travel times.

We download seismograms for events previously located from the Incorporated Research Institutions for Seismology (IRIS) and International Seismological Center (ISC) (On-Line Bulletin, 2014). We then pick our P and S-phases using Seismic Analysis Code (SAC) software and use these arrivals as the observed travel times (t_i^o).

After we pick the phases and ray trace to find predicted travel times, we plot the predicted and observed travel times. For example, Figures 9 and 10 compare observed and calculated times from a recorded and proposed earthquake. In figure 9, the observed times were recorded by TA stations in Louisiana after a M4.8 earthquake that occurred near Timpson, Texas. The calculated arrival times are ray traced from a proposed earthquake at 3.5 km depth to stations ranging from 10 to 400 km. The observed and calculated P and S-phases are plotted with the Borgfeldt East velocity model (Figure 9).

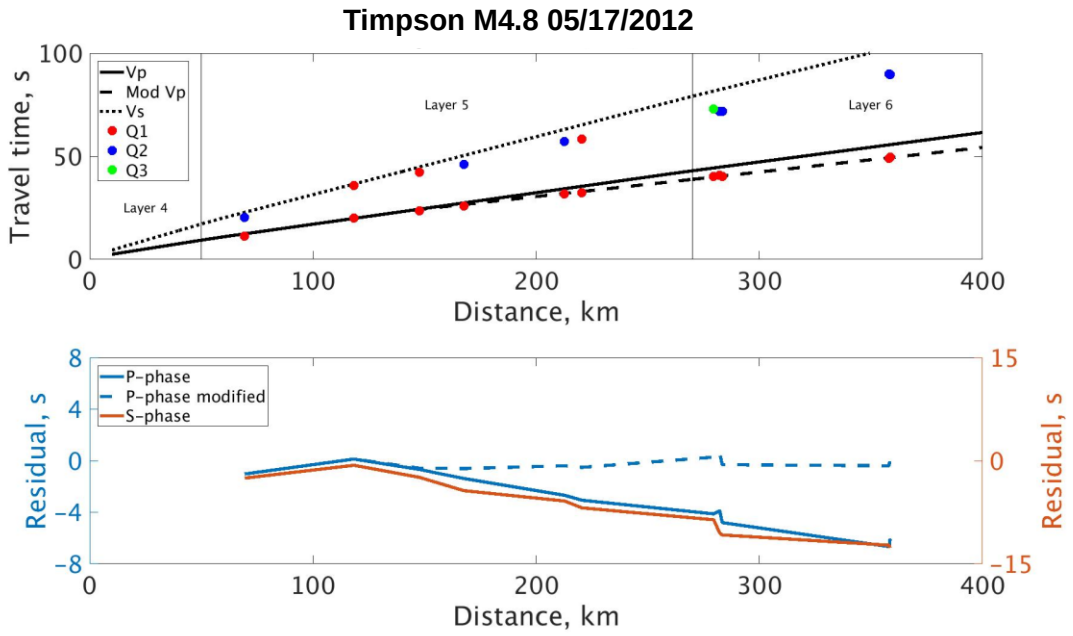

Figure 9: For the 17 May 2012 Timpson M4.8 earthquake, comparison of observed travel times with times calculated using the Borgfeldt East model. The top panel shows the travel time vs distance plots: circles are observed times – colors indicate quality of phase pick (red=Q1 (highest), blue=Q2, green=Q3); solid line is Borgfeldt East P-velocity model; dotted line is Borgfeldt East S-velocity model; dashed line is modified Borgfeldt East P-velocity model; vertical lines mark boundaries between layers of velocity which have the first arrival. Bottom panel shows residuals of observed travel times with respect to the P and S-velocity models.

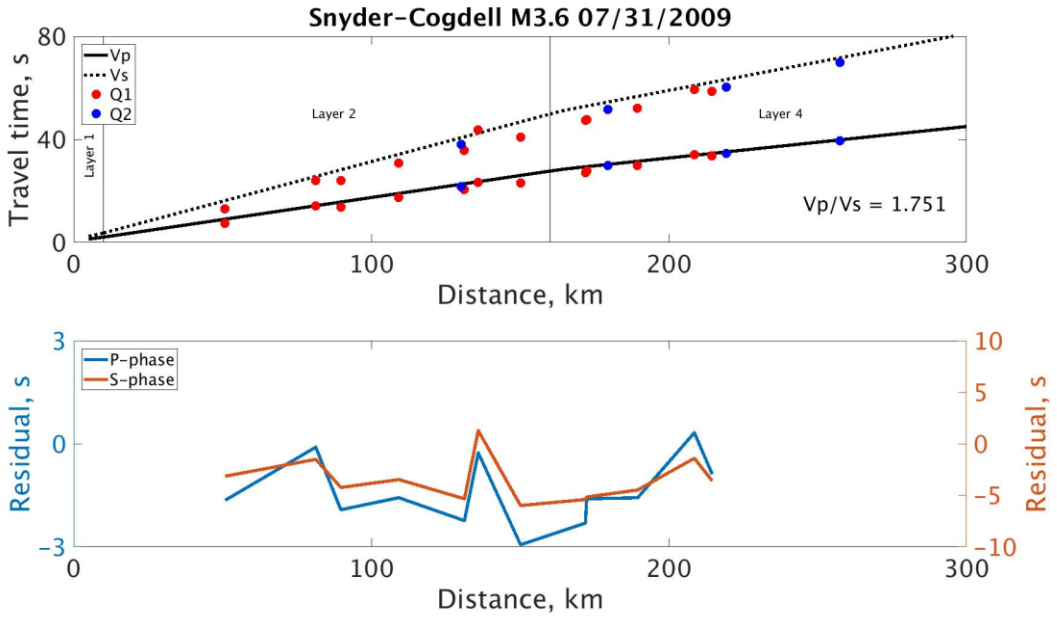

Figure 10: For the 31 July 2009 M3.6 Snyder-Cogdell earthquake, comparison of observed travel times with times calculated using the Ewing (1991) Midland Basin velocity model. The top panel shows the travel time vs distance plots: circles are observed times – colors indicate quality of phase pick (red=Q1 (highest), blue=Q2, green=Q3); solid line is Ewing P-velocity model; dotted line is S-velocity model with Vp/Vs=1.75; vertical lines mark boundaries between layers of velocity which have the first arrival. Bottom panel shows residuals of observed travel times with respect to the P and S-velocity models.

3.6 WADATI DIAGRAM

We use Wadati's (1928) method to determine the Vp/Vs ratio for the East, GCP, Panhandle and West regions. The FWB Vp/Vs is Frohlich *et al.*'s (2011) ratio determined from a Wadati diagram. The same earthquakes used as the observed P and S-phases for ray tracing are used to create Wadati diagrams for each region. After we pick the P and S phases for each event, we plot the travel time of the P phase against the difference in travel time between P and S. The slope of this line yields our Vp/Vs for each region (Table 2). These plots do not determine P and S-phase velocities but assume a constant Vp/Vs ratio.

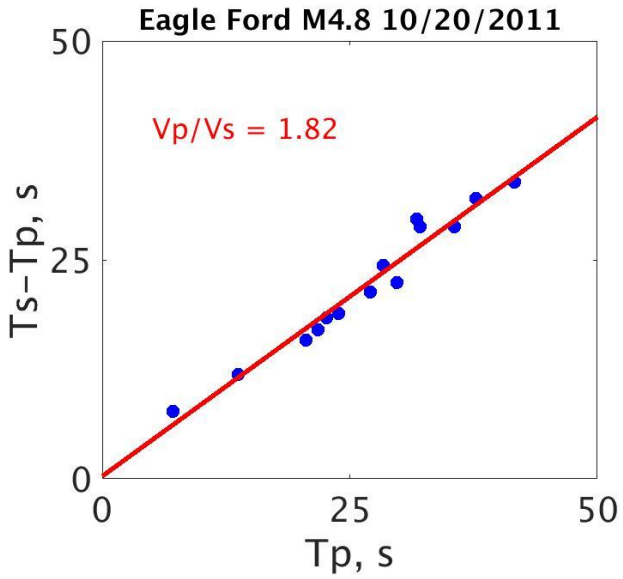

Figure 11: Wadati diagram for the Eagle Ford earthquake (10/20/2011, M4.8) in the GCP region. Red line is a least-squares fit to the phase arrival picks (blue circles) for stations that recorded the Eagle Ford event (Figure 12) and corresponds to a Vp/Vs ratio of 1.82.

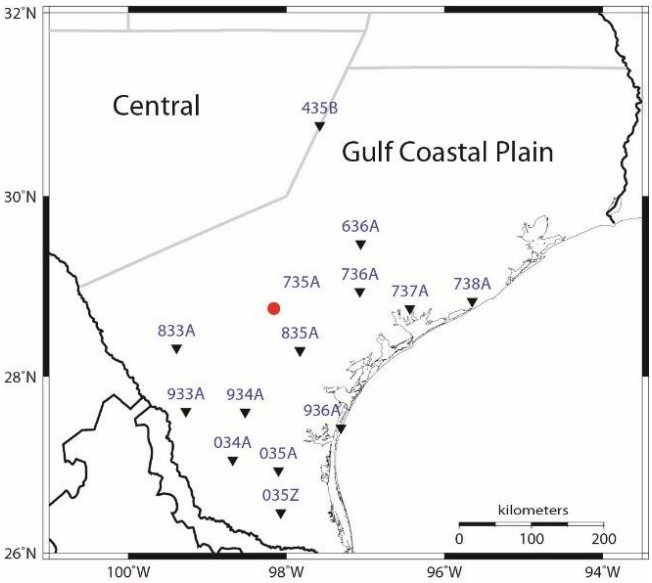

Figure 12: Map showing seismograph stations (triangles) where we picked P and S-phases for the Eagle Ford (10/20/2011, M4.8) earthquake (red circle) in the GCP. Labels indicate station codes.

Region	Event	Vp/Vs ratio	Reliable?
East	Timpson, M4.8, 05/17/2012	1.84	Y
Gulf Coastal Plain	Alice, M3.9, 04/25/2010	1.27	N
Gulf Coastal Plain	Eagle Ford M4.8, 10/20/2011	1.82	Y
Panhandle	Snyder-Cogdell M3.6, 07/31/2009	1.75	Y
West	M2.6, 12/28/2008	1.80	N

Table 2: Regional Vp/Vs ratios for each event for which we picked P and S-phases. If the event had reliable phase picks and high-quality data, we listed the event as reliable (Y) and used that value for the regional Vp/Vs ratio. If the phases were low quality and unreliable, we did not list the event as reliable (N) and did not use that Vp/Vs ratio for the region.

Chapter 4: Results

We present the preferred velocity models for each of our six regions. The preferred regional model: 1) produces a low RMS value for the regional earthquakes, and 2) is representative of the entire crust from surface to upper mantle. Figure 13 shows the preferred velocity models for each of the six regions.

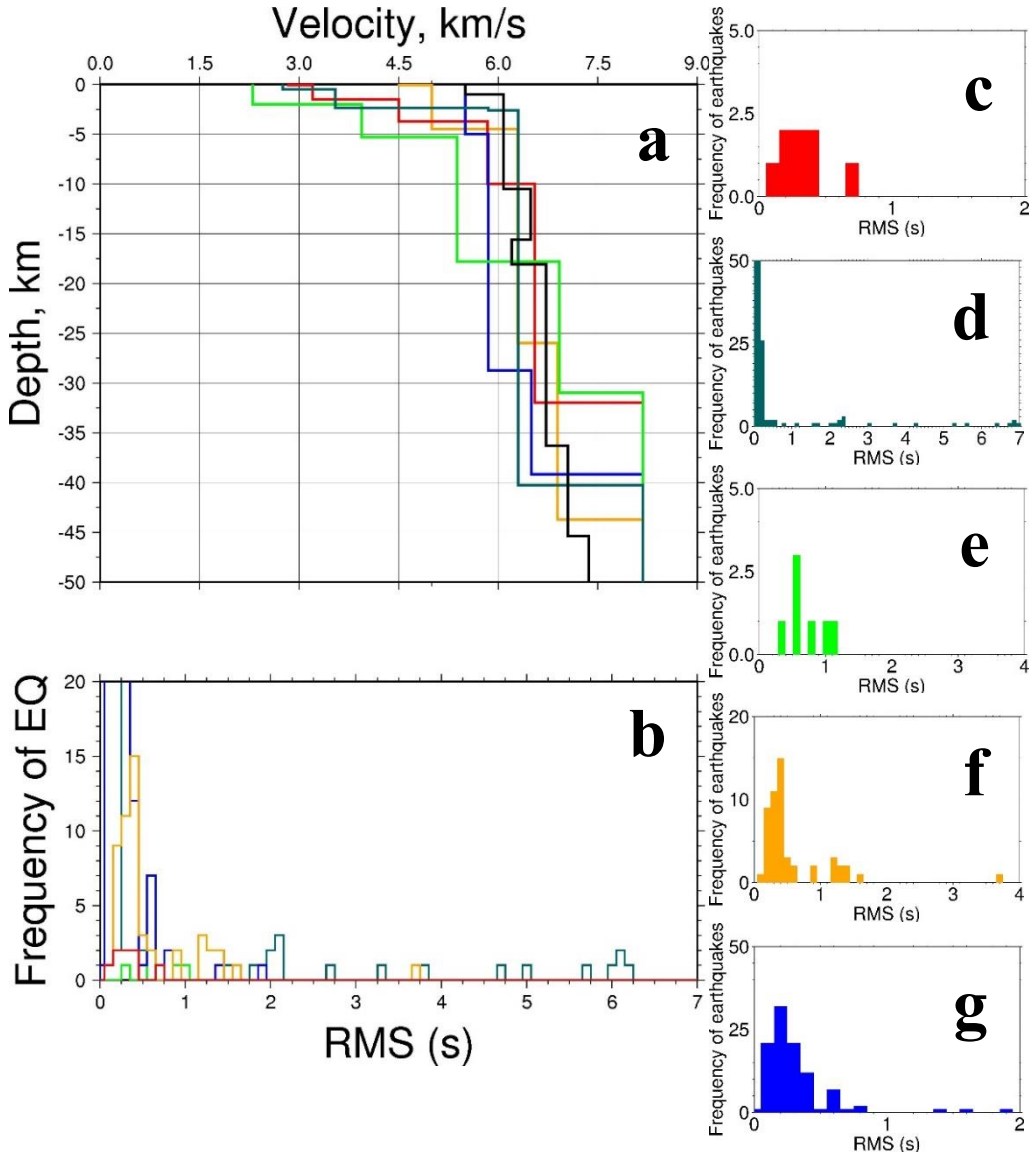

Figure 13: Figure A shows the six regional 1D preferred velocity models with depth. Figures B-G are histograms of the RMS values for the preferred velocity models. The colors in the figures are consistent: East - Borgfeldt East (red); Central – Mitchell and Landisman (1971) (black); FWB – modified Justinic et al. (2013) (dark green); GCP – Cram, Jr. (1961) (lime green); Panhandle – Borgfeldt Panhandle (orange); West – Borgfeldt Delaware Basin (blue).

4.1 EAST TEXAS

We test reference and newly generated velocity models with a set of eight regional earthquakes (Table 1; Figures 6 and 7) by relocating the events in HYPO1.40 at a fixed-depth of 5 km and with a constant Vp/Vs ratio. The preferred velocity model for East Texas is the Borgfeldt East model (Table 3), which generated an RMS value of 0.321 s. The preferred Vp/Vs ratio to apply to the entire velocity model is 1.84, determined from the Wadati diagram of the Timpson M4.8 earthquake (Figure E1).

Layers 1-4 (Table 3) are blocked velocities measured from the regional sonic logs (logs 1, 2, and 3) (Figure 5, Table B1). Layer 5 is equivalent to Layer 8 from Walter et al.'s (2016) velocity model. Layer 6 is representative of upper mantle material. The velocity (8.18 km/s) is the mantle velocity from Cram, Jr.'s (1961) velocity model, and the depth (32 km BSL) is the average crustal thickness in East Texas using EARS (Crotwell and Owens, 2005) data.

The preferred model's layers are constrained by sonic log data, ray tracing, RMS tests. Layers 1-4 are constrained by the digitized regional sonic logs (logs 1, 2, and 3) (Figure 5, Table B1). Layer 6 is constrained by EARS data. Layers 4-6 produced first arrivals when ray tracing from a proposed earthquake at 3.5 km depth, and are therefore constrained by RMS tests. Because the rays from layers 4-6 travel through shallower layers (1-3), layers 1-3 are constrained by RMS tests but less reliably than layers 4-6.

The average distance from source to receiver for the eight earthquakes used in regional RMS tests is 185.97 km; the minimum is 41.97 km, and the maximum is 363.13 km. These distances are contained in the ray trace of the Borgfeldt East model (Table 3) from a proposed earthquake at a depth of 3.5 km (Timpson event, Walter *et al.* (2016)) to stations 10 to 400 km away (Figure 9).

Borgfeldt East Texas

Layer	Vp (km/s)	Vs (km/s)	Thickness (km)	Depth BSL (km)
1	2.83	1.54	0.10	0.00
2	3.20	1.78	1.40	0.10
3	4.50	2.50	2.25	1.50
4	5.84	3.24	6.25	3.75
5	6.55	3.56	22.00	10.00
6	8.18	4.54	Halfspace	32.00

Table 3: Preferred velocity model for East Texas - Borgfeldt East with applied Vp/Vs ratio of 1.84.

4.2 FORT WORTH BASIN

We were provided analyst-picked events in the FWB by our colleagues at the Southern Methodist University. However, due to the clustering of the seismic activity in a few areas that are not well distributed throughout the region, we change the criteria to require only five P-phases. Although the reduced requirement of P-phases increases the spatial coverage of the events, the clustering does not allow us to test the velocities of the deeper crust for longer hypocenter to receiver ray paths. After eliminating the events that do not meet our criteria, we have a set of 616 events to test our FWB models (Figures 6 and S8).

We test reference and newly generated velocity models with the 616 regional earthquakes (Figures 6 and S8) by relocating the events in HYPO1.40 at a fixed-depth of 5 km and with a constant Vp/Vs ratio. The preferred velocity model for the FWB is a modified version of Justinic et al.'s (2013) velocity model (Table 4), which generated an RMS value of 0.190 s. The preferred Vp/Vs ratio to apply to the entire velocity model is 1.87, determined from Frohlich et al. (2011).

Layers 1-3 are the original Justinic et al. (2013) velocity model (Table A9), which is a three layer model based on Trigg No. 1 well near Cleburne, Texas. The top layer is a low-velocity layer based on proprietary data, the second is representative of the Pennsylvanian unit and the halfspace is representative of the Ordovician Ellenburger unit

and older rocks. The sonic logs we digitized and blocked for the FWB have overall higher velocities for the shallow crust (<5 km) in comparison to the Justinic *et al*. (2013) model (Table A9) but produced higher RMS values. Layer 4 is representative of the Ellenburger unit with the depth based on cross sections and previously tested SMU models.

The preferred model's layers are constrained by sonic log data, ray tracing, RMS tests. Layers 1 and 5 produced first arrivals when ray tracing from a proposed earthquake at 5 km depth. Therefore, layers 1 and 5 are constrained by RMS tests when relocating earthquakes. Because the rays are upgoing from layer 5, the velocities of the shallower layers (2-4) are also sampled but in a less significant sense than layers 1 and 5. Layers 2 and 3 are from the Justinic et al. (2013) model (Table A9) and layer 4 is based on regional geology but not well constrained.

The average distance from source to receiver for the 616 earthquakes used in regional RMS tests is 185.97 km; the minimum is 41.97 km, and the maximum is 363.13 km.

Modified Justinic et al. (2013)

Layer	Vp (km/s)	Vs (km/s)	Thickness (km)	Depth BSL (km)
1	2.75	1.47	0.50	0.00
2	3.54	1.89	1.87	0.50
3	5.85	3.13	0.23	2.37
4	6.30	3.37	37.68	2.60
5	8.18	4.37	Halfspace	40.28

Table 4: Preferred velocity model for FWB – modified Justinic *et al*. (2013) compressional velocity model with applied Vp/Vs ratio 1.87.

4.3 CENTRAL TEXAS

Since 2008, there have only been eight events within the Central Texas region and none meet the criteria to be used in RMS tests. Due to the paucity of data, we suggest that the Mitchell and Landisman (1971) model (Table A12) continue to be used as the preferred model for this region. Frohlich and Brunt (2013) used this model in their earthquake study of Eagle Ford seismicity and obtained reasonable results. Because the Eagle Ford events occurred near the Central Texas region and within similar geology, this is the best approximation for velocity structure in Central Texas.

4.4 GULF COASTAL PLAIN

We use seven earthquakes located within the GCP region and 1 º latitude of the boundaries. The Eagle Ford phases were picked by Frohlich and Brunt (2013). We test reference and newly generated velocity models with the set of seven regional earthquakes (Table 1; Figures 6 and S9) by relocating the events in HYPO1.40 at a fixed-depth of 5 km and with a constant Vp/Vs ratio. The preferred velocity model for the GCP is the Cram, Jr. (1961) model (Table 5), which generated an RMS value of 0.616 s. The preferred Vp/Vs ratio to apply to the entire velocity model is 1.82, determined from the Wadati diagram of the Eagle Ford M4.8 earthquake (Figure 11).

Layers 1 and 2 are representative of Cenozoic and Mesozoic sediments (Cram, Jr., 1961). Layer 3 is “Paleozoic and Precambrian metasediments and … igneous rocks” (Cram, Jr., 1961). Layer 4 is “… essentially oceanic crusts” (Cram, Jr., 1961). Layer 5 is “upper mantle material” (Cram, Jr., 1961).

The preferred model’s layers are constrained by geology, ray tracing, RMS tests. Layer 1 is constrained by geology. Layers 2-5 produced first arrivals when ray tracing from a proposed earthquake at 5 km depth, and are therefore constrained by RMS tests. Because

the rays from layers 2-5 pass through layer 1, layer 1 is also constrained by RMS tests but less reliably than layers 2-5.

The average distance from source to receiver for the seven earthquakes used in regional RMS tests is 561.94 km; the minimum is 15.31 km, and the maximum is 1,023.23 km. The ray trace of the Cram, Jr. (1961) model (Table 5) is from a proposed earthquake at a depth of 5 km (Eagle Ford event, Int. Seis. Cent.) to stations 10 to 300 km away (Figure D2).

Cram (1961)

Layer	Vp (km/s)	Vs (km/s)	Thickness (km)	Depth BSL (km)
1	2.30	1.26	2.00	0.00
2	3.94	2.16	5.30	2.00
3	5.38	2.96	12.50	7.30
4	6.92	3.80	13.20	19.80
5	8.18	4.49	Halfspace	33.00

Table 5: Preferred velocity model for GCP – Cram, Jr. (1961) compressional model (Table A13) with applied Vp/Vs ratio of 1.82.

4.5 PANHANDLE

We test reference and newly generated velocity models with a set of 51 regional earthquakes (Table 1; Figures 6 and S10) by relocating the events in HYPO1.40 at a fixed-depth of 5 km and with a constant Vp/Vs ratio. The preferred velocity model for the Panhandle is the Borgfeldt Panhandle model (Table 6), which generated an RMS value of 0.569 s. The preferred Vp/Vs ratio to apply to the entire velocity model is 1.75, determined from the Wadati diagram of the Snyder-Cogdell M3.6 earthquake (Figure E7).

Layer 1 is an average of blocked velocities measured from the regional sonic logs (logs 10, 11, 12) (Figure 5, Table B1). Layers 2-3 are from Mitchell and Landisman (1971)

(Table A12). Layer 4 is representative of upper mantle material. The velocity (8.18 km/s) is the Chelsea velocity model (Mitchell and Landisman, 1971), and the depth (42.72 km BSL) is the average crustal thickness in the Panhandle using EARS (Crotwell and Owens, 2005) data.

The preferred model's layers are constrained by sonic logs, receiver functions, ray tracing, and RMS tests. Layer 1 is constrained by the digitized regional sonic logs (logs 10, 11, 12) (Figure 5, Table B1). Layers 2 and 3 are from the Mitchell and Landisman (1971) (Table A12) velocity model from a refraction survey. Layer 4 is constrained by EARS data. Layers 1 and 4 produced first arrivals when ray tracing from a proposed earthquake at 5 km depth, and are therefore constrained by RMS tests. Because the rays from layer 4 pass through the shallower layers, layers 2 and 3 are also constrained by RMS test but less reliably than layers 1 and 4.

The average distance from source to receiver for the 51 earthquakes used in regional RMS tests is 367.69 km; the minimum is 20.61 km, and the maximum is 916.30 km. The ray trace of the Ewing (1991) model (Table 6) is from a proposed earthquake at a depth of 5 km to stations 10 to 300 km away (Figure 10).

Borgfeldt Panhandle

Layer	Vp (km/s)	Vs (km/s)	Thickness (km)	Depth BSL (km)
1	3.50	2.57	0.10	0.00
2	5.00	2.86	4.40	0.10
3	6.29	3.59	21.50	4.50
4	6.89	3.94	17.72	26.00
5	8.18	4.67	Halfspace	42.72

Table 6: Preferred velocity model for Panhandle – Borgfeldt Panhandle model with applied Vp/Vs ratio of 1.75.

4.6 WEST TEXAS

We test reference and newly generated velocity models with a set of 100 regional earthquakes (Table 1; Figures 6 and 8) by relocating the events in HYPO1.40 with free-depths and a constant Vp/Vs ratio. The preferred velocity model for West Texas is the Borgfeldt West model (Table 7), which generated an RMS value of 0.310 s. The preferred Vp/Vs ratio to apply to the entire velocity model is 1.75, determined from the Wadati diagram of the Snyder-Cogdell M3.6 earthquake (Figure E7).

Layers 1 and 2 are blocked velocities measured from the regional sonic logs (13, 14, 15, 16, 17) (Figure 5, Table B1) and are consistent with the Ewing (1991) cross-section, illustrating the basement top at approximately 4 km across the Delaware and Midland Basins. Layer 3 is a layer that was initially listed as an initial test velocity for the Hartse et al. (1992) velocity model. Layer 4 is representative of upper mantle material. The velocity (8.18 km/s) is the mantle velocity from Cram, Jr.'s (1961) velocity model, and the depth (39.17 km BSL) is the average crustal thickness in West Texas using EARS (Crotwell and Owens, 2005) data.

The preferred model's layers are constrained by sonic logs, receiver functions, ray tracing, and RMS tests. Layers 1 and 2 are constrained by the digitized regional sonic logs (13, 14, 15, 16, 17) (Figure 5, Table B1). Layer 4 is constrained by EARS data. Layers 1, 2, and 4 produced first arrivals when ray tracing from a proposed earthquake at 5 km depth. Therefore, layers 1, 2, and 4 are constrained by RMS tests when relocating earthquakes. Because the rays are upgoing from layer 4, the velocity of layer 3 is also sampled but in a less significant sense than layers 1, 2, and 4.

Borgfeldt Delaware Basin

Layer	Vp (km/s)	Vs (km/s)	Thickness (km)	Depth BSL (km)
1	5.50	3.06	5.00	0.00
2	5.85	3.25	23.75	5.00
3	6.50	3.61	10.42	28.75
4	8.18	4.54	Halfspace	39.17

Table 7: Possible preferred velocity model for West Texas – Borgfeldt model with applied Vp/Vs ratio of 1.75.

Chapter 5: Discussion

We tested new and reference velocity models for the six regions by relocating 782 regional events that met our earthquake criteria in HYPO1.40. We evaluated available velocity models for the state, generated new velocity models with an integration of available data, and provide six regional preferred models to use with the TexNet network based on available seismic data.

Our data allows us to generate new preferred regional velocity models for East Texas, Fort Worth Basin, Panhandle and West Texas. We confirm previously published models as the preferred models for the Gulf Coastal Plain and Central Texas. These models should serve as the regional reference models for purposes of earthquake location.

We used eight regional events to test the East Texas velocity models. The preferred regional model for East Texas is the Borgfeldt East Texas model (Table 3), which incorporates sonic log velocities, the layer 8 from Walter *et al.* (2016), EARS crustal thickness and Cram, Jr.'s mantle velocity. The layers are consistent with regional geology and previous crustal studies. Because of the relatively laminar geology, the 1D velocity model can serve as a relatively accurate representation of the crustal structure. There is constraint on model layers 1-4 by sonic log velocities. Model layers 4-6 are constrained by ray paths to the set of regional earthquakes located. The preferred Vp/Vs ratio to apply to the entire velocity model is 1.84. The Vp/Vs ratio is determined by a Wadati diagram of the Timpson M4.8 earthquake, which has recorded arrivals that constrain model layers 4-6. Borgfeldt East is a well constrained model, but future work could be done to improve the Vp/Vs ratio to apply to layers 1-3.

We used 616 regional events to test the FWB velocity models. The preferred regional model for the FWB is the modified Justinic *et al*. (2013) model (Table 4). Model layers 1-3 are the original Justinic et al. (2013) model. Model layer 4 is representative of the Ellenburger formation. Layer 5 is representative of upper mantle material and incorporates EARS crustal thickness and Cram, Jr. (1961) and Chelsea mantle velocity (Mitchell and Landisman, 1971). Due to the clustering of seismic stations and events in the

Dallas-Fort Worth metroplex area, only layers 1 and 5 are constrained by earthquake location tests. Model layer 4 is an approximation of geology, but future work with new seismic data will likely call for an additional layer between 4 and 5.

Central Texas does not have enough seismic or geophysical data to define a new velocity model. We suggest the continued use of the Mitchell and Landisman (1971) model (Table A12) with integration of new data that may become available.

We used seven regional earthquakes to test the GCP velocity models. The preferred regional model for the GCP is the Cram, Jr. (1961) model (Table 5), determined by refraction studies with representative geologic units. It produces the lowest RMS values (average 0.616 s) for the regional earthquakes and is representative of the crustal structure from surface to Moho. Layer 1 is constrained by the refraction study. Layers 2-5 are constrained by RMS tests as well as the refraction study. The preferred Vp/Vs ratio to apply to the entire model is 1.82, determined by a Wadati diagram of the Eagle Ford M4.8 earthquake (Figure 11). The distance between the source and receivers (35-255 km) for the Wadati diagrams correspond to travel time distances for layers 3-5 of the velocity model. Future work could be done to modify the Vp/Vs ratio for layers 1-2.

We used 51 regional earthquakes to test the Panhandle velocity models. The preferred regional model for the Panhandle is the Borgfeldt Panhandle model (Table 6), which incorporates sonic logs, layers 2 and 3 from Mitchell and Landisman (1971), the Chelsea and Cram, Jr. upper mantle velocity (Mitchell and Landisman, 1971; Cram, Jr., 1961), and EARS crustal thickness. It produces low RMS values (average=0.569 s) for the regional earthquakes and is representative of the crustal structure from surface to Moho. Layers 1 and 4 are constrained by RMS tests. Additionally, layers 1 and 4 are constrained by sonic logs and EARS data, respectively. The preferred Vp/Vs ratio to apply to the entire model is 1.75, generated from a Wadati diagram of the Snyder-Cogdell M3.6 earthquake (Figure E7). The distance between the source and receivers (50-257 km) for the Wadati diagrams corresponds to travel time distances for layers 2-3 of the velocity model. Future work could be done to modify the Vp/Vs ratio for layers 1 and 4.

The Midland Basin velocity structure published by Ewing (1991) (Table A16) is a potential velocity model for the Panhandle. This model generated a slightly lower average RMS value (0.565 s) than the Borgfeldt Panhandle model when relocating regional events, but the origin of the velocity structure is uncited and, therefore, not well constrained.

We used 100 regional earthquakes to test the West Texas velocity models. The preferred regional model for West Texas is the Borgfeldt Delaware Basin Average (BDBA) model (Table 7), which incorporates sonic log data, two layers from the Hartse, Sanford and Knapp (1992) model, and EARS crustal thickness. The simplicity of this regional model (four layers) is possibly due to the overall complexity in regional geology in West Texas. It produces low RMS values (average=0.310 s) for the regional earthquakes and is representative of the crustal structure from surface to Moho. Layers 1, 2, and 4 are constrained by RMS test. Layers 1 and 2 are also constrained by sonic log data. Layer 3 is not well constrained and could likely need modification with future seismic data. The preferred Vp/Vs ratio to apply to the entire model is 1.75, generated from a Wadati diagram of the Snyder-Cogdell M3.6 earthquake (Figure E7). The distance between source and receivers (50-257 km) for the Wadati diagram corresponds to travel time distances for layers 2 and 4 of the velocity model.

The Orr (1984) Keystone velocity model (Table A18) produced low RMS values as well (average=0.303 s), but is an incomplete model in terms of depth. This model has a half-space with the top at 3.4 km. Only layer 1 of this model is constrained by RMS tests, but the model is constrained by check-shot data. Future work could be done to determine if the Orr (1984) could be used in combination with the Borgfeldt BDBA model to refine the shallow layers.

Chapter 6: Conclusion

We tested and established six preferred regional 1D velocity models for Texas. Our study finds a new regional crustal seismic velocity model for East Texas, Fort Worth Basin, Panhandle and West Texas and confirms previously published velocity models for Central Texas and the Gulf Coastal Plain. These models synthesize geologic and geophysical data to provide the most accurate velocity model with lowest RMS travel time residuals for earthquake hypocenter location of regional events. We used P and S-wave arrival times recorded at seismometers installed before TexNet within each region to test and constrain the layers in each model.

The reduced residuals and agreement between ray tracing and phase arrivals can be attributed to more accurate seismic velocity models, and, therefore, a better model of the velocity structure. The preferred velocity model for East Texas is Borgfeldt east (Table 3) with a Vp/Vs ratio of 1.84. This model reduces the shallow crustal layers and updates the Moho depth and velocity. It is consistent with geologic cross-sections and studies. The preferred model for the Fort Worth Basin is the modified Justinic *et al.* (2013) model (Table 4) with a Vp/Vs ratio of 1.87. Due to the lack of seismic data, we suggest the Mitchell and Landisman (1971) model (Table A12) is the preferred model for the Central Texas region. The preferred model for the GCP is Cram, Jr.'s (1961) model (Table 5) with Vp/Vs ratio of 1.82. The preferred regional velocity model for the Panhandle is the Borgfeldt Panhandle model (Table 6) with a Vp/Vs ratio of 1.75. This is the preferred model because the RMS value is low and the velocity model is a complete representation of the velocity structure from surface to Moho. The preferred regional model for West Texas is the Borgfeldt West model (Table 7) with a Vp/Vs ratio of 1.75. This model could potentially be combined with the Orr (1984) model (Table A18).

We fixed the depths of all regional earthquakes for East, FWB, GCP and Panhandle at 5 km to ensure we tested the models with accurate epicenters and the error was not accommodated in the depth. Because we do not have controlled source seismic data, we

cannot do control tests on the velocity model locations. As more seismicity is recorded, the velocity models can be further refined.

The presented preferred regional velocity models of Texas are a statewide set of comprehensive 1D models for earthquake location studies within the state. With the reduction of RMS travel time residuals and relation to geologic units, we suggest the use of these preferred models as the regional velocity models for Texas with possible refinement with the addition of seismic data.

Appendix A

Frohlich et al. (2014)

Layer	Vp (km/s)	Thickness (km)	Depth BSL (km)
1	2.82	3.50	0.00
2	3.30	0.50	3.50
3	3.79	0.50	4.00
4	4.28	0.50	4.50
5	4.76	0.50	5.00
6	5.11	0.50	5.50
7	5.12	Halfspace	6.00

Table A1: East Texas reference model – Frohlich et al. (2014)

Walter et al. (2016)

Layer	Vp (km/s)	Thickness (km)	Depth BSL (km)
1	2.82	0.50	0.00
2	3.30	0.50	0.50
3	3.79	0.50	1.00
4	4.28	0.50	1.50
5	4.76	0.50	2.00
6	5.11	0.50	2.50
7	5.12	7.00	3.00
8	6.55	37.00	10.00
9	7.00	Halfspace	47.00

Table A2: East Texas reference model – Walter et al. (2016)

SMU - DFW

Layer	Vp (km/s)	Thickness (km)	Depth BSL (km)
1	2.90	0.60	-0.15
2	4.00	2.15	0.45
3	6.30	34.80	2.60
4	8.18	19.60	37.40
5	8.37	Halfspace	57.00

Table A3: Fort Worth Basin reference model – SMU DFW

SMU - Cleburne

Layer	Vp (km/s)	Thickness (km)	Depth BSL (km)
1	2.75	0.50	-0.25
2	3.54	1.85	0.25
3	5.85	37.90	2.10
4	8.18	17.00	40.00
5	8.37	Halfspace	57.00

Table A4: Fort Worth Basin reference model – SMU Cleburne

SMU - Irving

Layer	Vp (km/s)	Thickness (km)	Depth BSL (km)
1	2.90	0.60	-0.15
2	3.80	1.25	0.45
3	4.40	0.90	1.70
4	6.30	37.40	2.60
5	8.18	17.00	40.00
6	8.37	Halfspace	57.00

Table A5: Fort Worth Basin reference model – SMU Irving

SMU - Ouachita

Layer	Vp (km/s)	Thickness (km)	Depth BSL (km)
1	2.90	0.60	-0.15
2	4.40	0.55	0.45
3	5.00	1.60	1.00
4	6.30	37.40	2.60
5	8.18	17.00	40.00
6	8.37	Halfspace	57.00

Table A6: Fort Worth Basin reference model – SMU Ouachita

SMU - AzleEN

Layer	Vp (km/s)	Thickness (km)	Depth BSL (km)
1	3.03	0.185	-0.235
2	3.41	0.298	-0.050
3	4.02	0.843	0.248
4	4.12	0.610	1.091
5	5.18	0.064	1.701
6	5.09	0.855	1.765
7	6.15	37.38	2.620
8	8.18	17.00	40.00
9	8.37	Halfspace	57.00

Table A7: Fort Worth Basin reference model – SMU Azle

Hornbach et al. (2015)

Layer	Vp (km/s)	Thickness (km)	Depth BSL (km)
1	2.75	0.37	0.00
2	3.70	0.43	0.37
3	4.00	0.90	0.80
4	4.35	0.40	1.70
5	6.00	Halfspace	2.10

Table A8: Fort Worth Basin reference model – Hornbach et al. (2015)

Justinic et al. (2013)

Layer	Vp (km/s)	Thickness (km)	Depth BSL (km)
1	2.75	0.50	0.00
2	3.54	1.87	0.50
3	5.85	Halfspace	2.37

Table A9: Fort Worth Basin reference model – Justinic et al. (2013)

Frohlich et al. (2011)

Layer	Vp (km/s)	Thickness (km)	Depth BSL (km)
1	2.90	0.60	0.00
2	4.00	2.15	0.60
3	6.30	Halfspace	2.75

Table A10: Fort Worth Basin reference model – Frohlich et al. (2011)

Frohlich et al. (2012)

Layer	Vp (km/s)	Thickness (km)	Depth BSL (km)
1	2.90	0.60	0.00
2	4.00	2.15	0.60
3	6.30	15.00	2.75
4	8.00	Halfspace	17.75

Table A11: Fort Worth Basin reference model – Frohlich et al. (2012)

Mitchell and Landisman (1971) - Southwest Oklahoma Manitou model

Layer	Vp (km/s)	Thickness (km)	Depth BSL (km)
1	5.50	1.00	0.00
2	6.08	9.50	1.00
3	6.49	5.10	10.50
4	6.20	2.50	15.60
5	6.72	8.20	18.10
6	7.05	9.10	26.30
7	7.36	11.1	35.40
8	8.18	Halfspace	46.50

Table A12: Central Texas reference model – Mitchell and Landisman (1971)

Cram (1961)

Layer	Vp (km/s)	Vs (km/s)	Thickness (km)	Depth BSL (km)
1	2.30	1.26	2.00	0.00
2	3.94	2.16	5.30	2.00
3	5.38	2.96	12.50	7.30
4	6.92	3.80	13.20	19.80
5	8.18	4.49	Halfspace	33.00

Table A13: Gulf Coastal Plain reference model – Cram, Jr. (1961)

Keller and Shurbet (1975) - Tripartite 3

Layer	Vp (km/s)	Thickness (km)	Depth BSL (km)
1	2.20	3.00	0.00
2	3.80	6.00	3.00
3	5.30	9.00	9.00
4	6.50	13.50	18.00
5	7.80	Halfspace	31.50

Table A14: Gulf Coastal Plain reference model – Keller and Shurbet (1975) Manitou model

Mitchell and Landisman (1971) - Southwest Oklahoma Chelsea model

Layer	Vp (km/s)	Thickness (km)	Depth BSL (km)
1	4.00	0.60	0.00
2	6.05	0.40	0.60
3	5.50	2.10	1.00
4	6.08	10.30	3.10
5	6.49	3.00	13.40
6	6.20	1.50	16.40
7	6.72	8.20	17.90
8	7.05	9.10	26.10
9	7.36	11.10	35.20
10	8.18	Halfspace	46.30

Table A15: Panhandle reference model – Mitchell and Landisman (1971) Chelsea model

Ewing (1991) - Midland Basin

Layer	Vp (km/s)	Thickness (km)	Depth BSL (km)
1	6.14	12.00	0.00
2	6.51	6.00	12.00
3	6.20	5.00	18.00
4	6.72	9.00	23.00
5	7.10	8.00	32.00
6	7.35	10.00	40.00
7	8.23	Halfspace	50.00

Table A16: Panhandle reference model – Ewing (1991) Midland Basin

Ewing (1991) - Delaware Basin

Layer	Vp (km/s)	Thickness (km)	Depth BSL (km)
1	6.14	4.00	0.00
2	6.51	8.00	4.00
3	6.10	16.00	12.00
4	6.72	8.00	28.00
5	7.10	10.00	36.00
6	7.35	Halfspace	46.00

Table A17: West Texas reference model – Ewing (1991) Delaware Basin

Orr (1984) - Keystone, CBP

Layer	Vp (km/s)	Thickness (km)	Depth BSL (km)
1	4.70	0.40	0.00
2	4.86	0.55	0.40
3	4.98	1.25	0.95
4	5.17	1.10	2.20
5	5.39	0.10	3.30
6	6.07	Halfspace	3.40

Table A18: West Texas reference model – Orr (1984)

Stewart and Pakiser (1962) - Eastern New Mexico

Layer	Vp (km/s)	Thickness (km)	Depth BSL (km)
1	4.93	4.20	0.00
2	6.14	15.00	4.20
4	6.72	11.90	19.20
5	7.10	19.70	31.10
6	8.23	Halfspace	50.80

Table A19: West Texas reference model – Stewart and Pakiser (1962)

Appendix B

Region	API Number	ID
East Texas	42433200800000	1
	42073307460000	2
	42419309010000	3
Fort Worth Basin	42121330630000	4
	42497348180000	5
	42439300030000	6
Gulf Coastal Plain	4203927590000	7
	4229734682000	8
	4235533454000	9
Panhandle	4235930244000	10
	424833068000	11
	423933203500	12
West Texas	4238932245000	13
	4210931391000	14
	4238930423000	15
	4237131749000	16
	4249530306000	17

Table B1: List of API numbers for the sonic logs used in each region. The ID number corresponds to the ID used in location map and log plots.

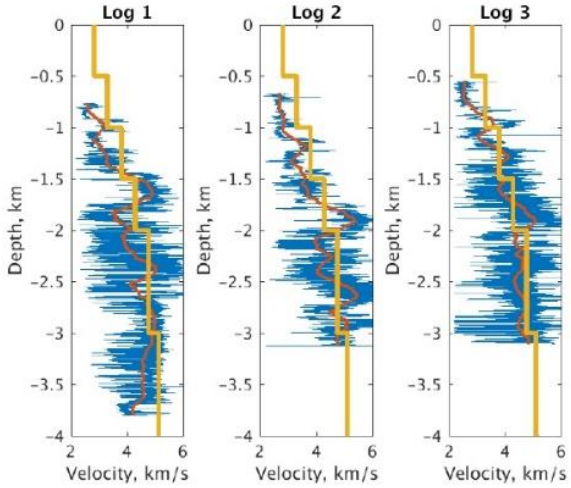

Figure B1: For East Texas region, digitized sonic logs (blue lines; Table B1) and Walter *et al.* (2016) (yellow) compressional velocity model (yellow line; see Table A2). Red lines are moving average of sonic logs.

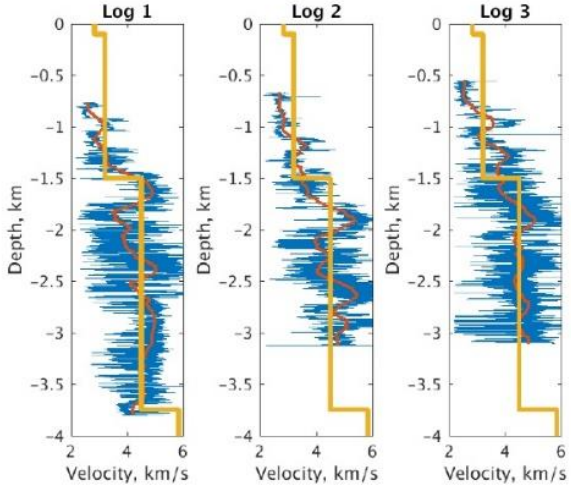

Figure B2: For East Texas region, digitized sonic logs (blue lines; Table B1) and Borgfeldt East (yellow) compressional velocity model (yellow line; see Table 3). Red lines are moving average of sonic logs.

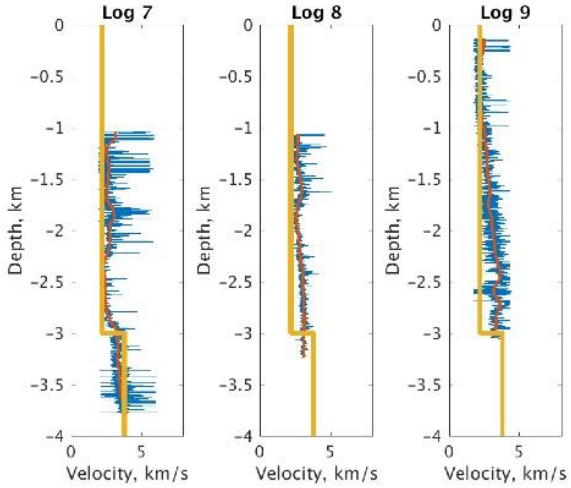

Figure B3: For Gulf Coastal Plain region, digitized sonic logs (blue lines; Table B1) and Keller and Shurbet (1975) compressional velocity model (yellow line; Table A14). Red lines are moving average of sonic logs.

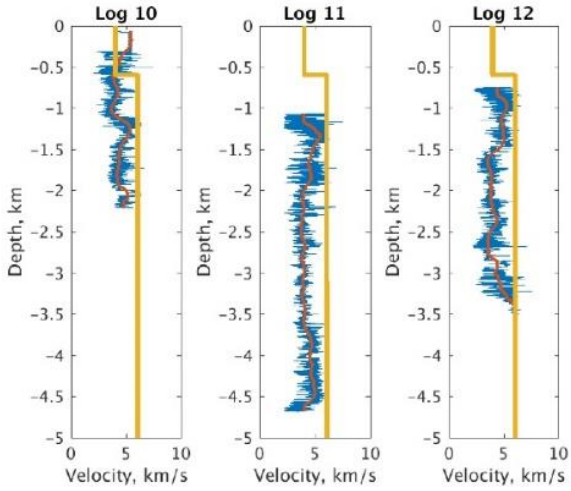

Figure B4: For Panhandle region, digitized sonic logs (blue lines; Table B1) and Mitchell and Landisman (1971) compressional velocity model (yellow line; Table A15). Red lines are moving average of sonic logs.

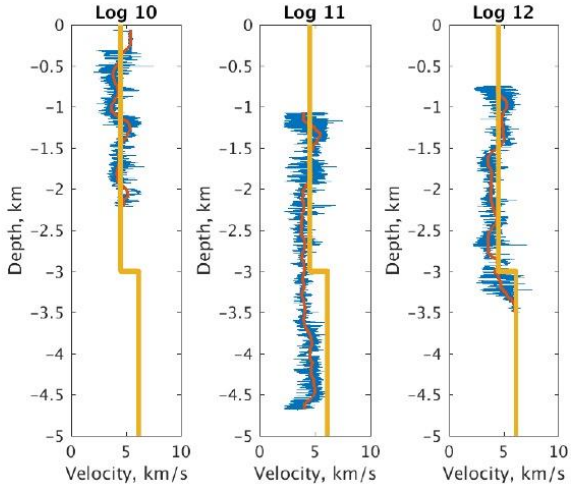

Figure B5: For Panhandle region, digitized sonic logs (blue lines; Table B1) and Ewing (1991) compressional velocity model (yellow line; Table A16). Red lines are moving average of sonic logs.

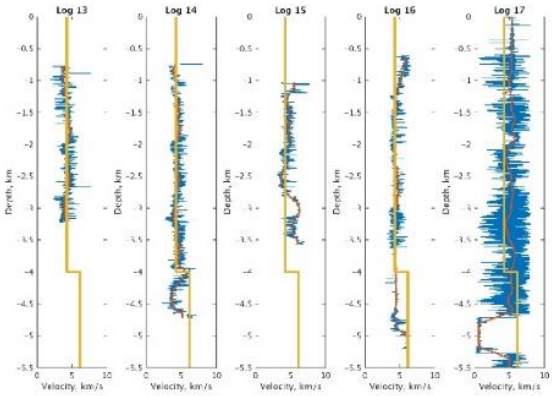

Figure B6: For West Texas region, digitized sonic logs (blue lines; Table B1) and Ewing (1991) compressional velocity model (yellow line; Table A17). Red lines are moving average of sonic logs.

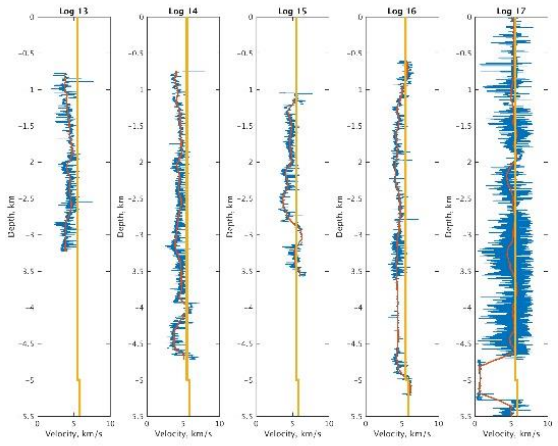

Figure B7: For West Texas region, digitized sonic logs (blue lines; Table B1) and Borgfeldt Delaware Basin model (yellow) compressional velocity model (yellow line; Table 6). Red lines are moving average of sonic logs.

Appendix C

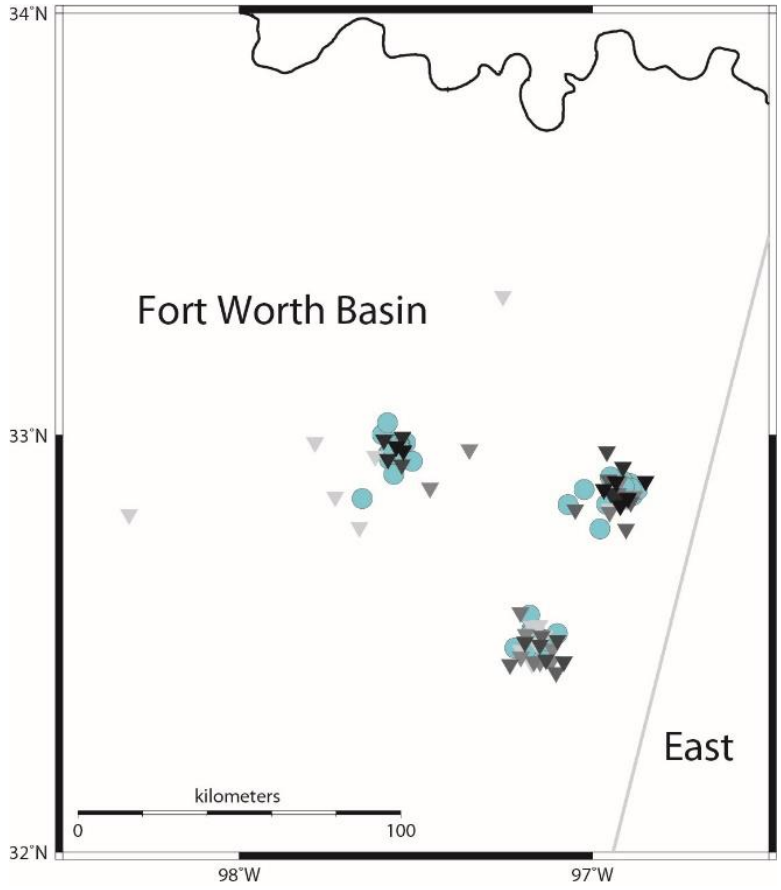

Figure C1: Map of the FWB region showing 616 earthquakes (turquoise circles) and seismograph stations (triangles) used for location test to assess regional velocity models. Earthquakes are events that occurred 2014-2016 having analyst-picked P and S-phases on records from local seismic networks, with epicenters determined using the modified Justinic *et al.* (2013) (Table 4). The triangles are seismograph stations that recorded phases for the mapped events. The darker the triangle, the more phases it recorded. Due to the clustering of the seismicity, this figure does not show the seismometers color coded.

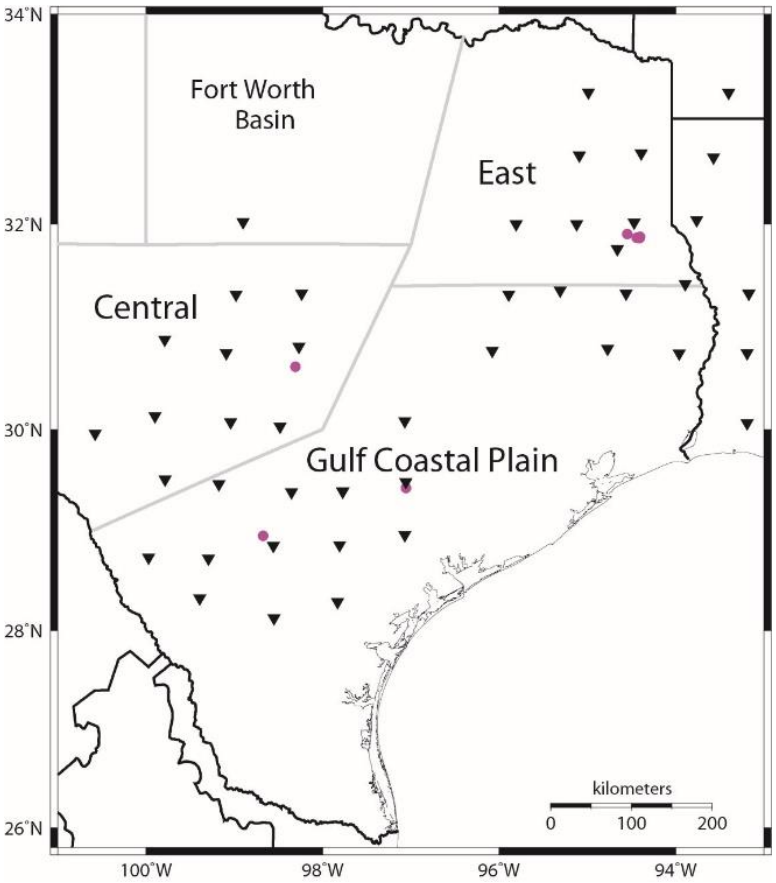

Figure C2: Map of the GCP region showing 7 earthquakes (purple circles) and seismograph stations (triangles) used for location test to assess regional velocity models. Earthquakes are events that occurred 2008-2010 having analyst-picked P and S-phases on records from Transportable Array stations, with epicenters determined using the Cram, Jr. (1961) model with applied Vp/Vs ratio (Table 5). The triangles are seismograph stations that recorded phases for the mapped events. Because there are so few events, the seismometers are the same color because each recorded between 1-6 phases.

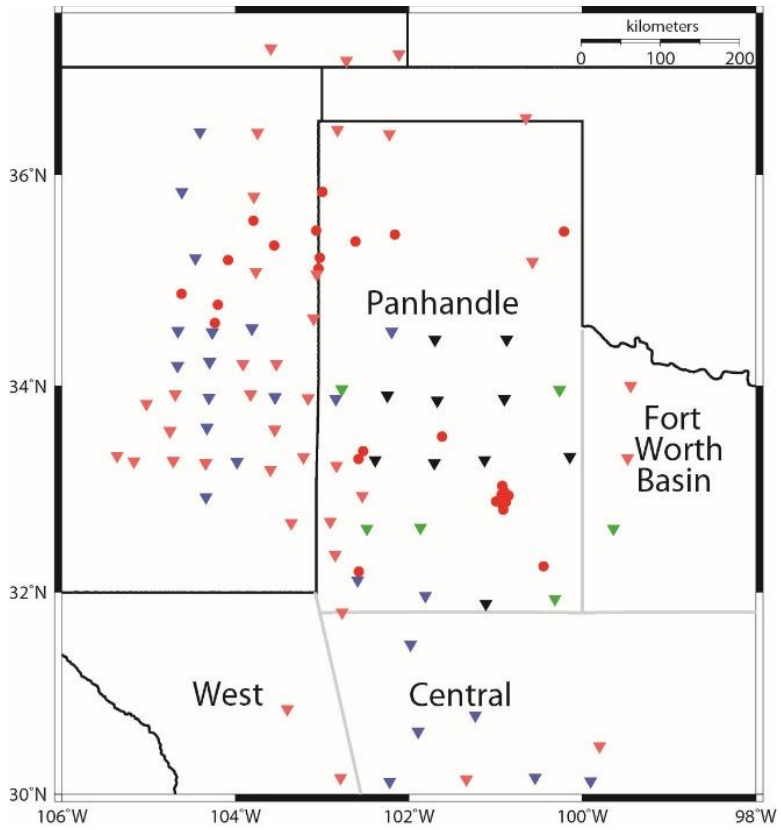

Figure C3: Map of the Panhandle region showing 53 earthquakes (red circles) and seismograph stations (triangles) used for location test to assess regional velocity models. Earthquakes are events that occurred 2008-2010 having analyst-picked P and S-phases on records from Transportable Array stations, with epicenters determined using the Ewing (1991) (Table A16). The triangles are seismograph stations that recorded phases for the mapped events (pink – fewer than 5 P-phases recorded; blue – 5-10 P-phases; maroon – 10-15 P-phases; green – 15-20 P-phases; black – greater than 20 P-phases).

Appendix D

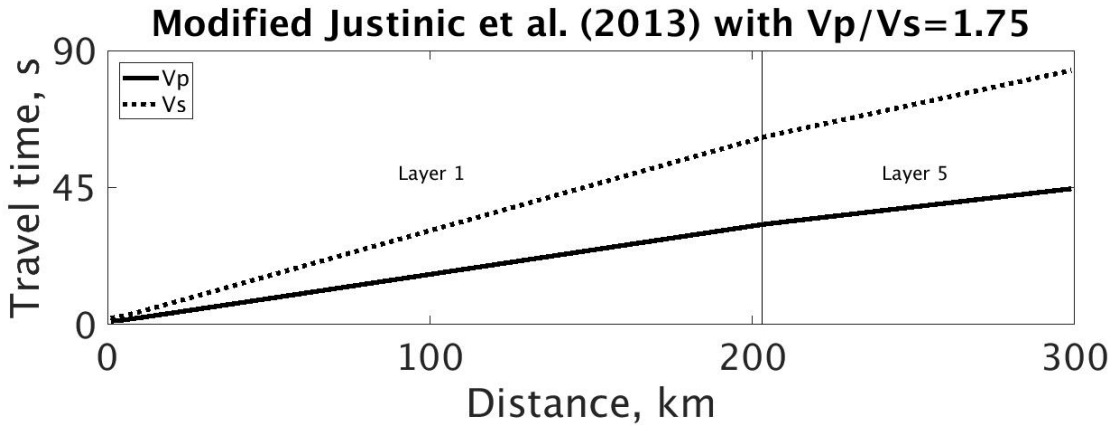

Figure D1: Calculated travel times using the modified Justinic *et al.* (2013) model (Table 4). Plot of P and S travel time vs distance: solid line is the modified Justinic *et al.* (2013) P-velocity model; dotted line is the modified Justinic *et al.* (2013) S-velocity model; vertical lines mark boundaries between layers of velocity which have the first arrival.

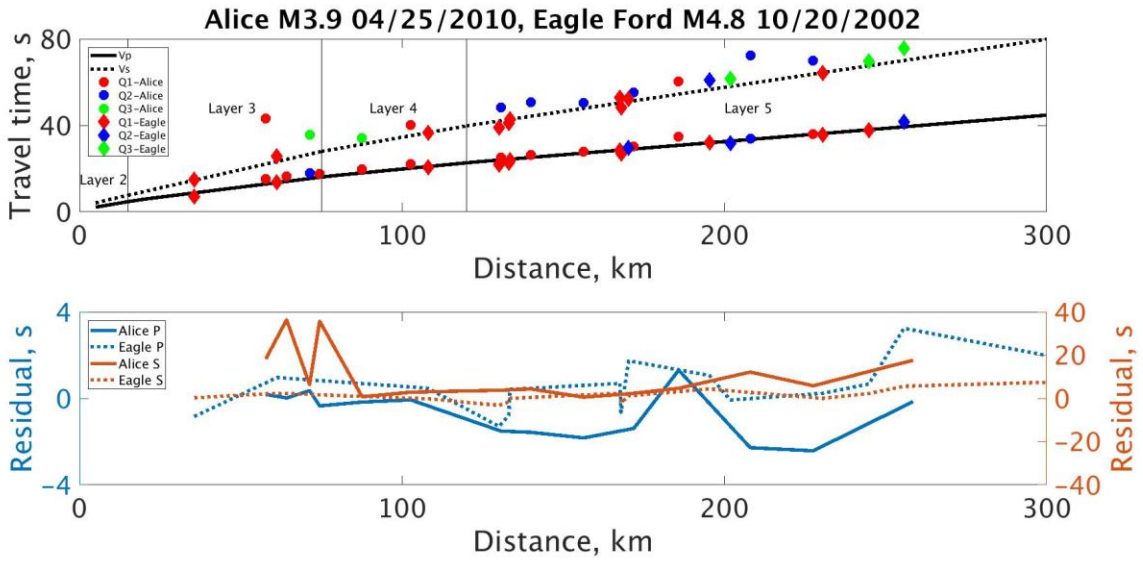

Figure D2: For of the 25 April 2010 Alice M3.9 earthquake, and 20 October 2011 Eagle Ford M4.8 earthquake, comparison of observed travel times with times calculated using the Cram, Jr. (1961) model (Table 5). The top panel plots the P and S travel time vs distance: circles are observed times of Alice earthquake and diamonds are Eagle Ford earthquake – colors indicate quality of phase pick (red=Q1 (highest), blue=Q2, green=Q3); solid line is Cram, Jr. (1961) P-velocity model; dotted line is Cram, Jr. (1961) S-velocity model; vertical lines mark boundaries between layers of velocity which have the first arrival. Bottom panel shows residuals of observed travel times with respect to the P and S-velocity models.

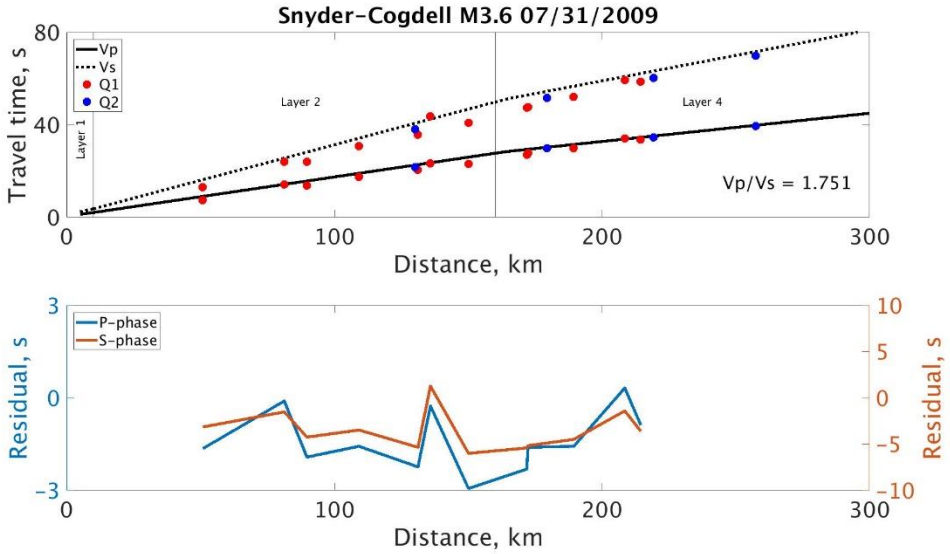

Figure D3: For the 31 July 2009 M3.6 Snyder-Cogdell earthquake, comparison of observed travel times with times calculated using the Borgfeldt West velocity model. The top panel shows the travel time vs distance plots: circles are observed times – colors indicate quality of phase pick (red=Q1 (highest), blue=Q2, green=Q3); solid line is Borgfeldt West P-velocity model; dotted line is S-velocity model with Vp/Vs=1.75; vertical lines mark boundaries between layers of velocity which have the first arrival. Bottom panel shows residuals of observed travel times with respect to the P and S-velocity models.

Appendix E

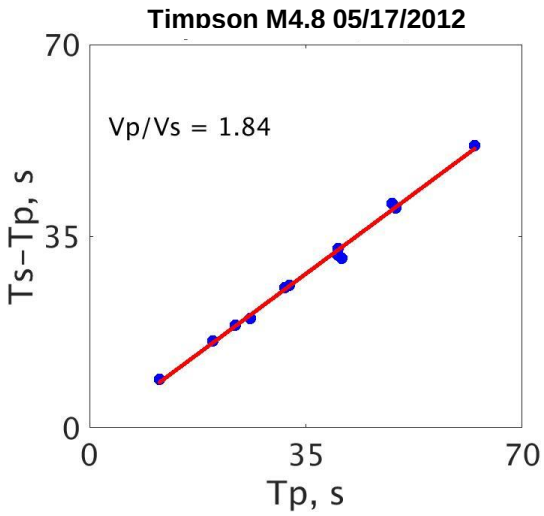

Figure E1: Wadati diagram for the Timpson earthquake (05/07/2012, M4.8) in the East Texas region. Red line is a least-squares fit to the phase arrival picks (blue circles) for stations that recorded the Timpson event (Figure E2) and corresponds to a Vp/Vs ratio of 1.84.

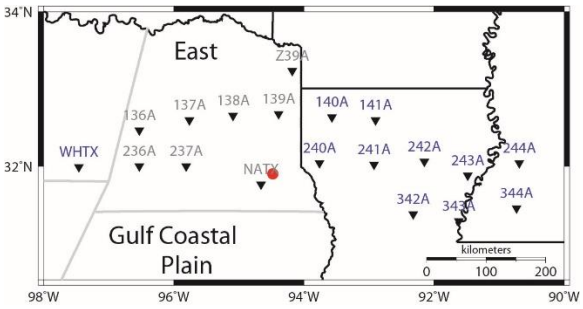

Figure E2: Map showing TA seismograph stations (triangles) that recorded P and S-phases of the Timpson earthquake (red circle) (05/07/2012, M4.8) in the East Texas region. The blue labeled stations indicate stations that recorded the event, and the grey labeled stations indicate stations that were not recording when the event occurred.

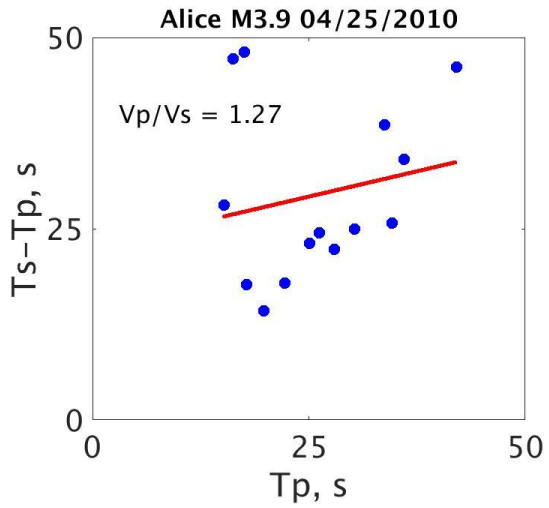

Figure E3: Wadati diagram for the Alice earthquake (04/25/2010, M3.9) in the GCP region. Red line is a least-squares fit to the phase arrival picks (blue circles) for stations that recorded the Alice event (Figure E4) and corresponds to a Vp/Vs ratio of 1.27.

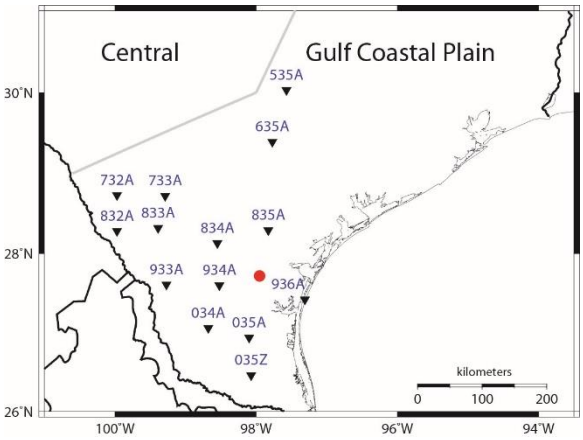

Figure E4: Map showing TA seismograph stations (triangles) that recorded P and S-phases of the Alice earthquake (red circle) (04/25/2010, M3.9) in the GCP region.

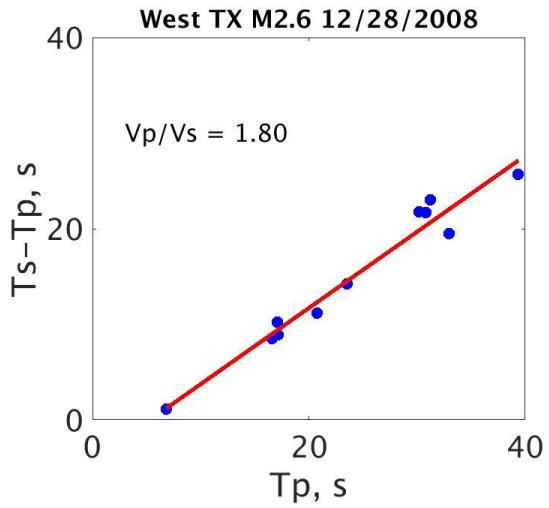

Figure E5: Wadati diagram for the west Texas earthquake (12/28/2008, M2.6) in the West Texas region. Red line is a least-squares fit to the phase arrival picks (blue circles) for stations that recorded the west Texas event (Figure E6) and corresponds to a Vp/Vs ratio of 1.80.

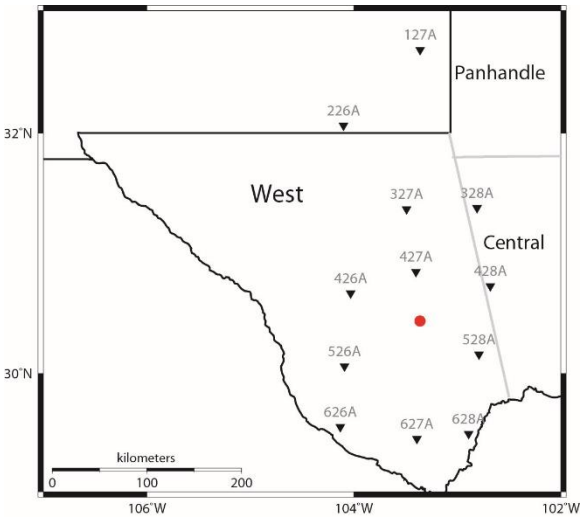

Figure E6: Map showing TA seismograph stations (triangles) that recorded P and S-phases of the M2.6 earthquake (blue circle) (12/28/2008, M2.6) in the Panhandle region.

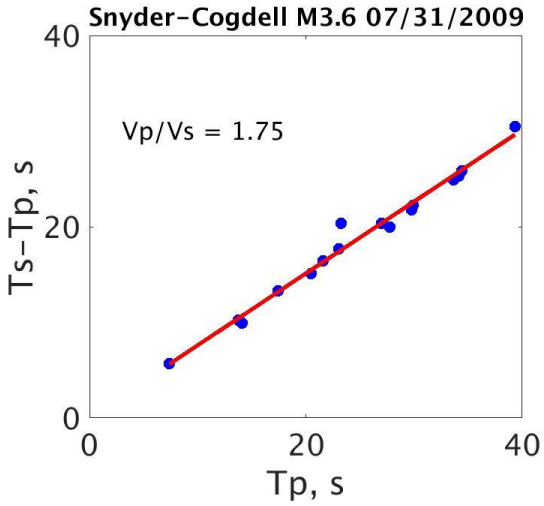

Figure E7: Wadati diagram for the Snyder-Cogdell earthquake (07/31/2009, M3.6) in the Panhandle region. Red line is a least-squares fit to the phase arrival picks (blue circles) for stations that recorded the Snyder-Cogdell event (Figure E8) and corresponds to a Vp/Vs ratio of 1.75.

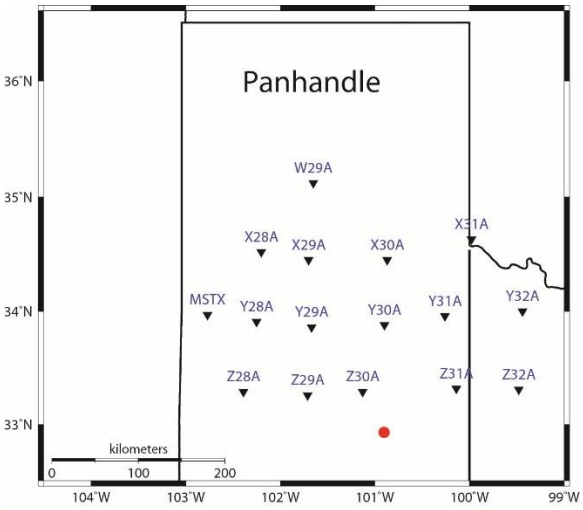

Figure E8: Map showing TA seismograph stations (triangles) that recorded P and S-phases of the Snyder-Cogdell earthquake (blue circle) (07/31/2009, M3.6) in the Panhandle region.

References

Cram Jr., I. H. (1961) 'A crustal structure refraction survey in South Texas', Geophysics, 26 (5), pp. 560–573.

Crotwell, H. P. and Owens, T. J. (2005) 'Automated receiver function processing', Seismological Research Letters2, 76, pp. 702–708.

Doser, D. I., Baker, M. R., Luo, M., Marroquin, P., Ballesteros, L., Kingwell, J., Diaz, H. L. and Kaip, G. (1992) 'The not so simple relationship between seismicity and oil production in the Permian Basin, west Texas', Pure and Applied Geophysics, 139 (3–4), pp. 481–506. doi: 10.1007/BF00879948.

Ewing, T. E. (1991) The Tectonic Framework of Texas. Edited by W. L. (The University of Texas at Austin, Fisher. Austin, Texas: Bureau of Economic Geology).

Ewing, T. E. (2016) Texas Through Time: Lone Star Geology, Landscapes, and Resources. Austin, Texas: University of Texas at Austin, Bureau of Economic Geology.

Frohlich, B. C., Deshon, H., Stump, B., Hayward, C., Hornbach, M. and Walter, J. I. (2016) 'A Historical Review of Induced Earthquakes in Texas', Seismological Research Letters, 87 (4), pp. 1–17. doi: 10.1785/0220160016.

Frohlich, C. (2012) 'Two-year survey comparing earthquake activity and injection-well locations in the Barnett Shale, Texas', Proceedings of the National Academy of Sciences, 109(35), pp. 13934–13938. doi: 10.1073/pnas.1207728109.

Frohlich, C. and Brunt, M. (2013) 'Two-year survey of earthquakes and injection/production wells in the Eagle Ford Shale, Texas, prior to the Mw 4.8 20 October 2011 earthquake', Earth and Planetary Science Letters. Elsevier B.V., 379, pp. 56–63. doi: 10.1016/j.epsl.2013.07.025.

Frohlich, C., Ellsworth, W., Brown, W. A., Brunt, M., Luetgert, J., Macdonald, T. and Walter, S. (2014) 'The 17 May 2012 M4.8 earthquake near Timpson, East Texas: An event possibly triggered by fluid injection', Journal of Geophysical Research: Solid Earth. doi: 10.1002/2013JB010755.

Frohlich, C., Glidewell, J. and Brunt, M. (2012) 'Location and felt reports for the 25 April 2010 m bLg 3.9 earthquake near Alice, Texas: Was it induced by petroleum production?', Bulletin of the Seismological Society of America, 102 (2), pp. 457–466. doi: 10.1785/0120110179.

Frohlich, C., Hayward, C., Stump, B. and Potter, E. (2011) 'The Dallas-Fort Worth earthquake sequence: October 2008 through May 2009', Bulletin of the

Seismological Society of America, 101 (1), pp. 327–340. doi: 10.1785/0120100131.

Gan, W. and Frohlich, C. (2013) 'Gas injection may have triggered earthquakes in the Cogdell oil field, Texas', Proceedings of the National Academy of Sciences, 110(47), pp. 18786–18791. doi: 10.1073/pnas.1311316110.

Geiger, L. (1912) 'Probability method for the determination of earthquake epicenters from the arrival time only', Bull. St. Louis Univ., 8, pp. 60–71.

Hales, A. L., Helsley, C. E. and Nation, J. B. (1970) 'Crustal Structure Study on Gulf Coast of Texas', AAPG Bulletin, 54 (11), pp. 2040–2057. Available at: http://archives.datapages.com/data/bulletns/1968-70/data/pg/0054/0011/2000/2040.htm.

Hammes, U. and Frébourg, G. (2012) 'Haynesville and Bossier mudrocks: A facies and sequence stratigraphic investigation, East Texas and Louisiana, USA', Marine and Petroleum Geology. Elsevier Ltd, 31 (1), pp. 8–26. doi: 10.1016/j.marpetgeo.2011.10.001.

Harry, D. L. and Londono, J. (2004) 'Structure and evolution of the central Gulf of Mexico continental margin and coastal plain, southeast United States', Geological Society of America Bulletin, 116 (1), p. 188. doi: 10.1130/B25237.1.

Hartse, H. E., Sanford, A. R. and Knapp, J. S. (1992) 'Incorporating Socorro magma body reflections into the earthquake location process', Bulletin of the Seismological Society of America, 82 (6), pp. 2511–2532. doi: 10.2113/gscanmin.39.5.1435.

Hermann, R. B., Benz, H. and Ammon, C. J. (2011) 'Monitoring the earthquake source process in North America', Bull. Seismol. Soc. Am., 101, pp. 2609–2625.

Hornbach, M. J., DeShon, H. R., Ellsworth, W. L., Stump, B. W., Hayward, C., Frohlich, C., Oldham, H. R., Olson, J. E., Magnani, M. B., Brokaw, C. and Luetgert, J. H. (2015) 'Causal factors for seismicity near Azle, Texas.', Nature communications. Nature Publishing Group, 6(6728), pp. 1–11. doi: 10.1038/ncomms7728.

Husen, S., Kissling, E. and Clinton, J. F. (2011) 'Local and regional minimum 1D models for earthquake location and data quality assessment in complex tectonic regions: Application to Switzerland', Swiss Journal of Geosciences, 104, pp. 455–469. doi: 10.1007/s00015-011-0071-3.

Husen, S., Kissling, E., Flueh, E. R. and Asch, G. (1999) 'Accurate hypocenter determination in the shallow part of the Nazca subduction zone in Northern Chile

using a combined on-/offshore network', Geophysics Journal Internal, 138, pp. 687–701.

Jackson, M. P. A. (1982) 'Fault tectonics of the East Texas Basin', Geological Circular - Texas, University, Bureau of Economic Geology, 82 (4), pp. 1–31.

Justinic, A. H., Stump, B., Hayward, C. and Frohlich, C. (2013) 'Analysis of the Cleburne, Texas, earthquake sequence from June 2009 to June 2010', Bulletin of the Seismological Society of America, 103 (6), pp. 3083–3093. doi: 10.1785/0120120336.

Keller, G. R. and Shurbet, D. H. (1975) 'Crustal Structure of the Texas Gulf Coastal Plain', Geological Society of America Bulletin, 86, pp. 807–810. doi: 10.1130/0016-7606(1975)86<807.

Mitchell, B. J. and Landisman, M. (1971) 'Geophysical measurements in the southern great plains', The structure and physical properties of the Earth's crust, pp. 77–93.

On-line Bulletin (2014) International Seismological Center. Available at: http://www.isc.ac.uk (Accessed: 15 March 2017).

Orr, C. D. (1984) A seismotectonic study and stress analysis of the Kermit Seismic Zone, Texas, The University of Texas at El Paso.

Sawyer, D. S., Buffler, R. T. and Pilger, R. H. (1991) 'The crust under the Gulf of Mexico', The Geology of North America, J. doi: 10.1130/DNAG-GNA-J.53.

Stewart, S. W. and Pakiser, L. C. (1962) 'Crustal structure in eastern New Mexico interpreted from the GNOME explosion', Bull. Seismol. Soc. Am., 52 (5), p. 1017–1030.

Tryggvason, E. and Qualls, B. R. (1967) 'Seismic refraction measurements of crustal structure in Oklahoma', Journal of Geophysical Research, 72 (14), pp. 3738–3740. doi: 10.1029/JZ072i014p03738.

Wadati, K. (1928). Shallow and deep earthquakes, *Geophys. Magazine* 1, pp. 161-202.

Walter, J. I., Dotray, P. J., Frohlich, C. and Gale, J. F. W. (2016) 'Earthquakes in Northwest Louisiana and the Texas–Louisiana Border Possibly Induced by Energy Resource Activities within the Haynesville Shale Play', Seismological Research Letters, 87(2A), pp. 285–294. doi: 10.1785/0220150193.

Vita

Taylor Borgfeldt was born in Goldsboro, North Carolina in 1993. She completed her B.S. in Geosciences at the University of Texas at Dallas in fall 2014. She began her M.S. at the University of Texas at Austin in summer 2015. Upon completion of her M.S. in Geosciences from UT, she will begin work at GSI Environmental.

Permanent email: tborgfeldt1@gmail.com
This thesis was typed by Taylor Borgfeldt.